G. Bor *et al.* (2018) "Tire Tracks and Integrable Curve Evolution,"
International Mathematics Research Notices, Vol. 00, No. 0, pp. 1–71
Advance Access publication on Month XX, 20XX
doi:10.1093/imrn/rny087

Downloaded from https://academic.oup.com/imrn/advance-article-abstract/doi/10.1093/imrn/rny087/4998816 by Pennsylvania State University user on 15 January 2019

Tire Tracks and Integrable Curve Evolution

Gil Bor[1], **Mark Levi**[2], **Ron Perline**[3], **and Sergei Tabachnikov**[4,*]

[1]CIMAT, A.P. 402, Guanjuato, Gto. 36000, Mexico, [2]Department of Mathematics, Penn State, University Park, PA 16802, USA, [3]Department of Mathematics, Drexel University, 3141 Chestnut Street, Philadelphia, PA 19104, USA, and [4]Department of Mathematics, Penn State, University Park, PA 16802, USA

[*]*Correspondence to be sent to: email: tabachni@math.psu.edu*

We study a simple model of bicycle motion: a segment of fixed length in multi-dimensional Euclidean space, moving so that the velocity of the rear end is always aligned with the segment. If the front track is prescribed, the trajectory of the rear wheel is uniquely determined via a certain first order differential equation—the bicycle equation. The same model, in dimension two, describes another mechanical device, the hatchet planimeter. Here is a sampler of our results. We express the linearized flow of the bicycle equation in terms of the geometry of the rear track; in dimension three, for closed front and rear tracks, this is a version of the Berry phase formula. We show that in all dimensions a sufficiently long bicycle also serves as a planimeter: it measures, approximately, the area bivector defined by the closed front track. We prove that the bicycle equation also describes rolling, without slipping and twisting, of hyperbolic space along Euclidean space. We relate the bicycle problem with two completely integrable systems: the Ablowitz, Kaup, Newell, and Segur (AKNS) system and the vortex filament equation. We show that "bicycle correspondence" of space curves (front tracks sharing a common back track) is a special case of a Darboux transformation associated with the AKNS system. We show that the filament hierarchy, encoded as a single generating equation, describes a three-dimensional bike of imaginary length.

Received July 14, 2017; Revised March 9, 2018; Accepted April 13, 2018
Communicated by Prof. Igor Rivin

© The Author(s) 2018. Published by Oxford University Press. All rights reserved. For permissions, please e-mail: journals.permission@oup.com.

We show that a series of examples of "ambiguous" closed bicycle curves (front tracks admitting self bicycle correspondence), found recently F. Wegner, are buckled rings, or solitons of the planar filament equation. As a case study, we give a detailed analysis of such curves, arising from bicycle correspondence with multiply traversed circles.

1 Introduction

This paper concerns a simple model for bicycle motion. An idealized bike is an oriented segment of fixed length that moves in such a way that the velocity of the rear end is aligned with the segment: the rear bicycle wheel is fixed on its frame, whereas the front wheel can steer, see Figure 1. The same "no skid" non-holonomic constraint describes the bicycle motion in $\mathbb{R}^n$ (and, more generally, in any Riemannian manifold; e.g., hyperbolic and elliptic spaces).

The bicycle model. The bicycle model has attracted much attention in recent years, due in part to its unexpected relations with other mathematical problems, old and new. We start with a brief description of these relations and recent work on this bicycle model.

If the front track is prescribed, the trajectory of the rear wheel is uniquely determined, once the initial orientation of the bicycle is chosen, via a certain first order differential equation, the *bicycle equation* (equation (4) of Section 2). In dimension two, this equation is equivalent to the much studied stationary Schrödinger, or Hill, equation $\ddot{x} + p(t)x = 0$, whose potential $p(t)$ depends on the geometry of the front track and the length of the bicycle [33, 34].

The bicycle monodromy. Associated with any given front track (closed or not), one defines the *bicycle monodromy*, that is, the map $S^{n-1} \to S^{n-1}$ which assigns to each initial orientation of the bike its final orientation once the front wheel completes its

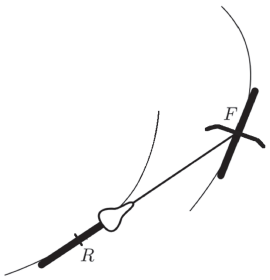

Fig. 1. The bicycle front and rear tracks.

Downloaded from https://academic.oup.com/imrn/advance-article-abstract/doi/10.1093/imrn/rny087/4998816 by Pennsylvania State University user on 15 January 2019

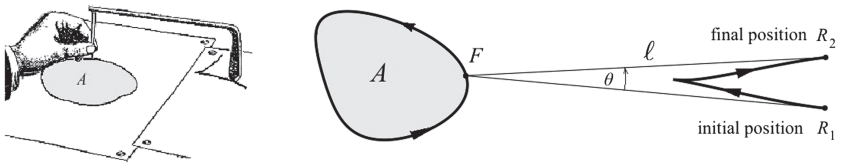

Fig. 2. The hatchet planimeter.

travel. In dimension two, Foote [17] observed that this map is a Möbius transformation; this observation was extended to $\mathbb{R}^n$ in [35]; we give a new proof in Theorem 3.

The hatchet planimeter and Menzin's conjecture. The bicycle model in dimension two describes also a device, known as the hatchet (or Prytz) planimeter, for measuring areas of planar domains. The hatchet planimeter consists of a rod with a hatchet blade fixed at one end and a pointed pin at the other, as shown in Figure 2. To measure the area of a planar region, one traces its boundary with the pin; the hatchet slides on the paper without sideslip, behaving like the rear wheel of a bike.

The angle θ between the hatchet's initial and final orientations gives an approximation of the area A of the region, with an error of order $O(1/\ell)$,

$$A = \ell^2\theta + O(1/\ell), \tag{1}$$

where ℓ is the hatchet's length, see [17, 18, 26]. A natural question is whether this formula is an approximation to some exact result. In Section 2.7 we show that indeed θ is an approximation to the solid angle of a certain cone in $\mathbb{R}^3$.

Planimeters were popular objects of mathematical study some 100 years ago. In particular, Menzin (1906) conjectured that if $A > \pi\ell^2$ then the monodromy has a fixed point (i.e., for a particular initial orientation of the planimeter the trajectory of the blade is closed). In other words, the monodromy is a hyperbolic element of the Möbius group $\mathrm{PSL}_2(\mathbb{R})$. This conjecture was proved in [35]; see [18, 38] for expository accounts and [27] for a version of this theorem in spherical and hyperbolic geometries.

Bicycle correspondence. A closed rear track determines *two* front tracks (one riding forward and the other backward relative to some chosen direction of the rear track). These two front tracks are said to be in *bicycle correspondence*. See Figure 3.

Bicycle correspondence of curves has a number of remarkable properties: it satisfies the so-called Bianchi permutability and it preserves the conjugacy class of the bicycle monodromy (with an arbitrary length of the bicycle, not only the one that defines

Downloaded from https://academic.oup.com/imrn/advance-article-abstract/doi/10.1093/imrn/rny087/4998816 by Pennsylvania State University user on 15 January 2019

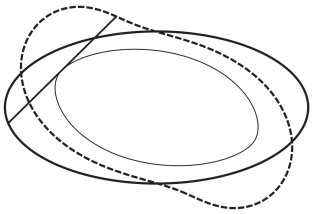

Fig. 3. The heavy and dotted curves are in bicycle correspondence; the thin curve is their common back track.

the bicycle correspondence), see [47, 48] and Section 3.1 below. As a result, bicycle correspondence has infinitely many conserved quantities, starting with the perimeter.

In dimension three, bicycle correspondence is intimately related to the well-studied *filament (a.k.a. binormal, smoke ring, localized induction) equation*, a completely integrable dynamical system on the space of smooth closed curves in $\mathbb{R}^3$, equivalent to the nonlinear Schrödinger equation via the Hashimoto transformation [25]. Bicycle correspondence is the Darboux–Bäcklund transformation of the filament equation; it commutes with the flow of the filament equation and shares with it its integrals and an invariant symplectic structure [48].

Zindler curves. An interesting problem is whether one can determine the direction of motion given closed rear and front tracks of a bicycle. Usually, this is possible, but sometimes it is not (e.g., if the tracks are concentric circles), see [16]. The front track in such an ambiguous pair of curves is in bicycle correspondence with itself; in other words, two points, x and y, can traverse this curve in such a way that the distance $|xy|$ remains constant and the velocity of the midpoint of the segment xy is aligned with this segment. Let us call the curves with this property *Zindler curves* (see [56] and Figure 4).

Incidentally, Zindler curves provide solutions to another problem, Ulam's problem in flotation theory ([43], problem 19): which bodies float in equilibrium in all positions? In the two-dimensional case, the boundary of such a body is a Zindler curve. (See [5, 41, 42] for early work and [23] for historical information; in particular, about Herman Auerbach, 1901–1942). Recently, a wealth of results concerning this problem was obtained in [6, 7, 46] and in a series of papers by F. Wegner [50]–[55]. Wegner constructed a family of nontrivial Zindler curves (he did not use this terminology), described explicitly in terms of elliptic functions. He was motivated by a study of the motion of an electron in a magnetic field whose strength depends quadratically on the

Downloaded from https://academic.oup.com/imrn/advance-article-abstract/doi/10.1093/imrn/rny087/4998816 by Pennsylvania State University user on 15 January 2019

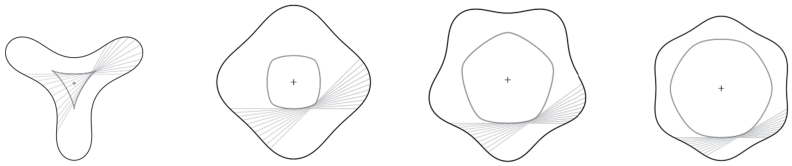

Fig. 4. Examples of Zindler curves from [55].

distance to the origin. The "three problems" in [55] are the ambiguous tire track problem, Ulam's flotation problem, and the motion of an electron.

A full description of planar Zindler curves, let alone their higher-dimensional version, is still unknown. Let us also mention a discrete version of the bicycle correspondence and, in particular, a polygonal version of Zindler curves [46, 47].

Plan of the paper. In Section 2 we discuss various forms of the bicycle differential equation (most of them appeared previously in the literature), paying special attention to the most interesting two- and three-dimensional cases, and give a new proof that the bicycle monodromy is a Möbius transformation (Theorems 1–3). Our goal here is to present a unified, group-theoretic, approach to these foundational matters.

The geometry of bike tracks in $\mathbb{R}^2$ is greatly clarified by extension of the problem to $\mathbb{R}^3$; without such extension some phenomena remain hidden. Theorem 4 (stated for any dimension) is a new result: it describes the derivative of the bicycle monodromy at a fixed point in terms of the geometry of the corresponding closed rear track. In dimension three, one has the Berry phase formula (Corollary 2.19): the derivative in question is a complex number whose modulus depends on the signed length of the rear track and whose argument is the Hannay angle, that is, the area on the unit sphere bounded by the tangent Gauss image of the rear track. This fact is then used to explain geometrically, via Berry's phase, why the planimeter works. A two-dimensional version of the formula for the derivative of the monodromy at the fixed point was obtained in [35].

As we mentioned earlier, in the planar case, a sufficiently long bicycle serves as a planimeter. In Theorem 5, we show that a similar fact holds in higher dimensions: the bicycle measures, approximately, the area *bivector*, determined by the front track.

Theorem 6 of Section 2 gives yet another interpretation of the bicycle equation: this equation describes rolling, without slipping and twisting, of the hyperbolic space along Euclidean space, with the front track being the trajectory of the contact point. This interpretation fits naturally with the fact that the bicycle monodromy is a Möbius transformation, an isometry of the hyperbolic space.

Downloaded from https://academic.oup.com/imrn/advance-article-abstract/doi/10.1093/imrn/rny087/4998816 by Pennsylvania State University user on 15 January 2019

Section 3 is concerned with the relation of the bicycle problem with the *filament equation*. The equation defines a flow on the space of smooth closed curves in $\mathbb{R}^3$, a completely integrable Hamiltonian system, part of an infinite hierarchy of pairwise commuting Hamiltonian vector fields. We start with a detailed description of the notion of bicycle correspondence between curves and give a new proof that this correspondence preserves the conjugacy class of the bicycle monodromy (Theorem 7). The filament equation shares with the bicycle equation its invariance under bicycle correspondence, known as the Darboux, or Bäcklund, transformation, in the context of the filament equation.

In Section 3.2, we encode the filament hierarchy in a single equation with a formal parameter and show (Corollary 3.14) that this equation coincides with the equation of a three-dimensional bike of *imaginary length*.

Given a closed front bicycle track, it is intuitively clear that if the length of the bicycle is infinitesimal, then there exist two closed trajectories of the bicycle, corresponding to the bicycle near-tangent to the front track, pointing either forward or backward. Proposition 3.15 provides a rigorous analysis of this phenomenon in dimension three. As a result, in Theorem 8, we obtain an infinite collection of integrals of the bicycle correspondence that, conjecturally, coincide with the known integrals of the filament equation (the Hamiltonians of the commuting hierarchy of vector fileds).

The classical Bernoulli elastica are extrema of the total squared curvature functional among curves with fixed length. *Buckled rings* (or *pressurized elastica*) are plane curves that are extrema of the total squared curvature functional, subject to length and area constraints. In Section 3.3, we prove that the curves, constructed by Wegner, are buckled rings (Theorem 9). This provides a connection with the planar filament equation, another completely integrable system, a close relative of the (three-dimensional) filament equation: buckled rings are solitons of the planar filament equation, that is, evolve under its flow by isometries.

Section 4 provides a detailed study of a family of Zindler curves, the ones in bicycle correspondence with multiply-traversed circles (Theorem 10).

The paper is concluded with two appendices: in appendix A we describe a relation of the bicycle equation with yet another integrable system: the Ablowitz, Kaup, Newell, and Segur (AKNS) system. We show (Theorem 12) that the bicycle correspondence in dimension three can be thought of as a special case of a Darboux transformation associated with the AKNS system. In appendix B we provide a proof of the main analytical tool (Proposition 3.15) needed to establish the existence of the integrals of the bicycle correspondence of Theorem 8.

Downloaded from https://academic.oup.com/imrn/advance-article-abstract/doi/10.1093/imrn/rny087/4998816 by Pennsylvania State University user on 15 January 2019

2 The Bicycle Equation and Its Monodromy

2.1 The bicycle equation

We consider a smoothly parametrized curve $\Gamma(t)$ in $\mathbb{R}^n$ (the "front track"), and a real number $\ell > 0$ (the "bicycle length"); a rear track γ is, by the definition, any parametrized curve $\gamma(t)$ in $\mathbb{R}^n$ that satisfies

$$\|\Gamma(t) - \gamma(t)\| = \ell, \tag{2}$$

$$\gamma(t) - \Gamma(t) \text{ is tangent to } \gamma \text{ at } \gamma(t). \tag{3}$$

To keep track of the direction of the rear wheel relative to the front wheel, we introduce the unit direction vector $\mathbf{r}(t) \in S^{n-1}$ (see Figure 5), thus rewriting condition (2), expressing the bicycle "rigidity" condition, as $\gamma(t) = \Gamma(t) + \ell\mathbf{r}(t)$. Condition (3), expressing the rear wheel "no-skid" condition, is then equivalent to an ordinary differential equation for $\mathbf{r}(t)$ which we now state.

Proposition 2.1. Let $\Gamma(t), \mathbf{r}(t)$ be parameterized curves in $\mathbb{R}^n, S^{n-1}$, respectively, $\ell > 0$, and $\gamma(t) = \Gamma(t) + \ell\mathbf{r}(t)$. Then the "no-skid" condition (3) is equivalent to

$$\ell\dot{\mathbf{r}} = -\mathbf{v} + (\mathbf{v} \cdot \mathbf{r})\mathbf{r}, \tag{4}$$

where $\mathbf{v} = \dot{\Gamma}$ and where $\cdot$ denotes the scalar product.

Equation (4) is the ℓ-bicycle equation in $\mathbb{R}^n$, defined for every parametrized front track $\Gamma(t)$ and bicycle length ℓ.

Proof. Let us decompose $\mathbf{v} = \dot{\Gamma}$ as $\mathbf{v} = \mathbf{v}^{\parallel} + \mathbf{v}^{\perp}$, where $\mathbf{v}^{\parallel}, \mathbf{v}^{\perp}$ are the orthogonal projections of $\mathbf{v}$ onto $\mathbb{R}\mathbf{r}$, $\mathbf{r}^{\perp}$, respectively, as in Figure 6. Then conditions (2)–(3) are

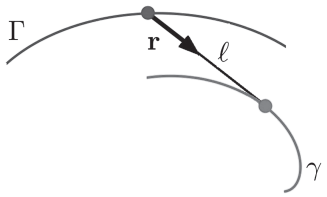

Fig. 5. The bicycling "no skid" condition.

Downloaded from https://academic.oup.com/imrn/advance-article-abstract/doi/10.1093/imrn/rny087/4998816 by Pennsylvania State University user on 15 January 2019

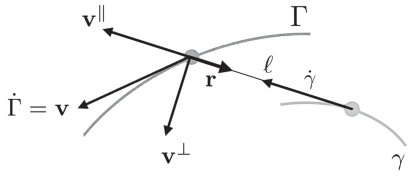

Fig. 6. The proof of Proposition 2.1.

equivalent to $\dot\gamma = \mathbf{v}^{\parallel}$. From $\gamma = \Gamma + \ell\mathbf{r}$ follows $\dot\gamma = \mathbf{v} + \ell\dot{\mathbf{r}}$, hence $\dot\gamma = \mathbf{v}^{\parallel}$ is equivalent to $0 = \mathbf{v}^{\perp} + \ell\dot{\mathbf{r}}$. Now $\mathbf{v}^{\perp} = \mathbf{v} - \mathbf{v}^{\parallel} = \mathbf{v} - (\mathbf{v}\cdot\mathbf{r})\mathbf{r}$, from which (4) follows. ■

Remark 2.2. Equation (4) was derived above for $\mathbf{r}(t) \in S^{n-1}$ and indeed it leaves invariant the condition $\|\mathbf{r}\| = 1$, as can be easily checked. But it makes sense also for arbitrary $\mathbf{r}(t) \in \mathbb{R}^n$, for which it has also an interesting mechanical interpretation, at least in the $\|\mathbf{r}\| < 1$ case (see Section 2.10 below).

Remark 2.3. Even if Γ is a regularly immersed curve, that is, $\dot\Gamma$ does not vanish, $\dot\gamma$ may vanish. From (4), we see that $\dot\gamma = \mathbf{v} + \ell\dot{\mathbf{r}}$ vanishes precisely when $\mathbf{v}\cdot\mathbf{r} = 0$, that is, when the bicycle is perpendicular to the front wheel track Γ.

In the planar case, the resulting singularities of γ are generically semi-cubical cusps (see [35], Section 2, for more information).

The conceptual explanation of the singularities is as follows (this explanation can be safely skipped at first reading). The configuration space of oriented segments of length ℓ in $\mathbb{R}^n$ is the spherization of the tangent bundle $ST\mathbb{R}^n$, and the non-holonomic "no-skid" constraint defines a completely non-integrable n-dimensional distribution $\mathscr{D}$ therein. The motion of the bicycle is a smooth curve in $ST\mathbb{R}^n$ tangent to the distribution $\mathscr{D}$ (i.e., a horizontal curve relative to the distribution).

The two projections $ST\mathbb{R}^n \to \mathbb{R}^n$, to the front and rear ends of the segment, yield the front and rear bicycle tracks, see Figure 7. The former projection is transverse to $\mathscr{D}$, therefore the front track is a smooth curve, but the kernel of the latter projection is contained in $\mathscr{D}$, and hence the rear track may have singularities; this happens when the horizontal curve is tangent to this kernel.

2.2 The bicycle monodromy

Given a parameterized curve $\Gamma(t)$ in $\mathbb{R}^n$, consider the family of unit spheres centered at points of Γ, and identify these spheres with each other by parallel translation (such an

Downloaded from https://academic.oup.com/imrn/advance-article-abstract/doi/10.1093/imrn/rny087/4998816 by Pennsylvania State University user on 15 January 2019

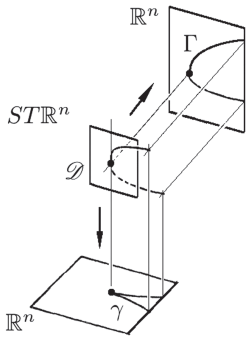

Fig. 7. The two projections $ST\mathbb{R}^n \to \mathbb{R}^n$.

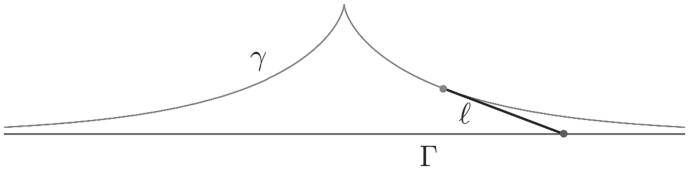

Fig. 8. The tractrix.

identification is assumed throughout the paper). Fix a point $\Gamma(t_0)$ on the curve Γ. Then, according to Proposition 2.1, conditions (2) and (3) define, for each t (for which $\Gamma(t)$ is defined) and $\ell > 0$, a diffeomorphism

$$M_\ell^t : S^{n-1} \to S^{n-1},$$

called *the bicycle monodromy*, that maps $\mathbf{r}_0$ to $\mathbf{r}(t)$, where $\mathbf{r}(t)$ is the solution to (4) satisfying the initial condition $\mathbf{r}(t_0) = \mathbf{r}_0$. In other words, M_ℓ^t is the flow of the differential equation (4).

Example 2.4. (See Figure 8) Let Γ be the x-axis in $\mathbb{R}^2$, parameterized by $\Gamma(t) = (t, 0)$. Substitute $\mathbf{r} = (\cos\theta, \sin\theta)$ in (4), where $\theta = \theta(t)$, and obtain $\ell\dot{\theta} = \sin\theta$. Another substitution $p = \tan(\theta/2)$ linearizes this equation, yielding $\ell\dot{p} = p$, with solution $p(t) = p_0 e^{t/\ell}$. The resulting rear track γ is the classical *tractrix*, and we can use the solution $p(t)$ to give it an explicit parametrization (see, e.g., [17] for details).

Downloaded from https://academic.oup.com/imrn/advance-article-abstract/doi/10.1093/imrn/rny087/4998816 by Pennsylvania State University user on 15 January 2019

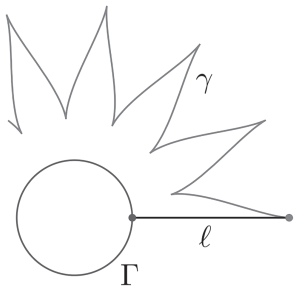

Fig. 9. The circular tractrix.

Example 2.5. (See Figure 9) Let Γ be the unit circle in $\mathbb{R}^2$, parameterized by $\Gamma(t) = (\cos t, \sin t)$. As in the previous example, substitute $\mathbf{r} = (\cos\theta, \sin\theta)$ in (4), giving $\ell\dot{\theta} = -\cos(\theta - t)$. Changing to $\phi := \theta - t$ gives $\dot{\phi} = -1 - (\cos\phi)/\ell$. Changing again to $p := \tan(\phi/2)$ gives

$$\dot{p} = -\frac{1}{2\ell}\left[p^2(\ell - 1) + \ell + 1\right].$$

This is a constant coefficient Riccati equation that can be solved explicitly in elementary functions (see Section 4 below for details).

2.3 Bicycling in $\mathbb{R}^2$

There are a number of reformulations of (4) for $n = 2$ found in the literature [15, 17, 18, 35, 46]. We collect them in this subsection.

First, we use an angle coordinate θ on S^1, that is, substitute $\mathbf{r} = (\cos\theta, \sin\theta)$ in (4), obtaining,

$$\ell\dot{\theta} = v_1 \sin\theta - v_2 \cos\theta, \qquad \dot{\Gamma} = (v_1, v_2). \tag{5}$$

Now the *projective coordinate* $p = \tan(\theta/2)$, that is, the slope of a vector with the argument $\theta/2$, satisfies the *Riccati equation*

$$\dot{p} = \frac{1}{2\ell}\left(-v_2 + 2v_1 p + v_2 p^2\right), \qquad \dot{\Gamma} = (v_1, v_2). \tag{6}$$

A consequence of (6) is the following theorem of Foote [17].

Downloaded from https://academic.oup.com/imrn/advance-article-abstract/doi/10.1093/imrn/rny087/4998816 by Pennsylvania State University user on 15 January 2019

Downloaded from https://academic.oup.com/imrn/advance-article-abstract/doi/10.1093/imrn/rny087/4998816 by Pennsylvania State University user on 15 January 2019

Theorem 1. The flow of (5) is the projection to S^1 of the flow of the linear system

$$\begin{pmatrix}\dot{x}\\ \dot{y}\end{pmatrix} = -\frac{1}{2\ell}\begin{pmatrix}v_1 & v_2\\ v_2 & -v_1\end{pmatrix}\begin{pmatrix}x\\ y\end{pmatrix} \tag{7}$$

via the double covering map (using complex notation) $z = x + iy \mapsto \mathbf{r} = z^2/|z|^2$ or, more explicitly,

$$(x, y) \mapsto \mathbf{r} = \left(\frac{x^2 - y^2}{x^2 + y^2}, \frac{2xy}{x^2 + y^2}\right).$$

Thus the bicycle monodromy for $n = 2$ is given by elements of the Möbius group $\mathrm{PSL}_2(\mathbb{R})$ of fractional linear transformations $p \mapsto (ap + b)/(cp + d)$.

Proof. It is well-known that the flow of a Riccati equation consists of Möbius transformations (see, e.g., [28], p. 24). Let us review the argument. Consider the linear system

$$\begin{pmatrix}\dot{x}\\ \dot{y}\end{pmatrix} = \begin{pmatrix}a & b\\ c & -a\end{pmatrix}\begin{pmatrix}x\\ y\end{pmatrix}. \tag{8}$$

One can check easily that a solution $(x(t), y(t))$ of this system projects to a solution $p(t) = y(t)/x(t)$ of the equation

$$\dot{p} = c - 2ap - bp^2. \tag{9}$$

Thus the flow of the Riccati equation (9) is the projectivization of the flow of the linear system (8). Applying this procedure to (7), we obtain (6), and thus (5). ■

The next reformulation of (4) is obtained by switching to a *moving frame* along Γ (the Frenet–Serret frame). To this end, assume first that Γ is parameterized by arc length, so that $\mathbf{v} = \dot{\Gamma}$ is a unit tangent vector along Γ. Complete $\mathbf{v}$ to a positively oriented orthonormal frame $\{\mathbf{v}, \mathbf{n}\}$ along Γ. Then $\dot{\mathbf{v}} = \kappa\mathbf{n}$, where κ is the curvature function along Γ. Now we use an angle coordinate Θ for $\mathbf{r}$ in the moving frame $\{\mathbf{v}, \mathbf{n}\}$, that is, let $\mathbf{r} = e^{i\Theta}\mathbf{v} = (\cos\Theta)\mathbf{v} + (\sin\Theta)\mathbf{n}$. (Note: the angle Θ is π minus the "steering angle" α of [35].)

Proposition 2.6. $\mathbf{r} = e^{i\Theta}\mathbf{v}$ satisfies (4) for $n = 2$ if and only if $\Theta(t)$ satisfies

$$\dot{\Theta} = \frac{\sin\Theta}{\ell} - \kappa.$$

Using the projective coordinate $P = \tan(\Theta/2)$, the last equation is equivalent to

$$\dot{P} = \frac{P}{\ell} - \frac{\kappa}{2}(1 + P^2), \tag{10}$$

which is the projectivization $P = Y/X$ of the linear system

$$\begin{pmatrix} \dot{X} \\ \dot{Y} \end{pmatrix} = \frac{1}{2} \begin{pmatrix} -1/\ell & \kappa \\ -\kappa & 1/\ell \end{pmatrix} \begin{pmatrix} X \\ Y \end{pmatrix}.$$

The proof is a direct calculation, and we omit it.

2.4 Bicycling in $\mathbb{R}^3$

Similar to the $n = 2$ case, equation (4) for $n = 3$ can be reformulated in a variety of ways. To begin with, we rewrite (4) for $n = 3$ using the vector product in $\mathbb{R}^3$.

Lemma 2.7. Equation (4), for $n = 3$, is equivalent to

$$\dot{\mathbf{r}} = \frac{1}{\ell}(\mathbf{v} \times \mathbf{r}) \times \mathbf{r}, \quad \mathbf{v} = \dot{\Gamma}. \tag{11}$$

We omit the simple verification.

Next we rewrite (11) as a *complex* Riccati equation, that is, as the projectivization of a two-dimensional complex linear system.

Theorem 2. The flow of (11) is the projection to S^2 of the flow of the complex linear system

$$\begin{pmatrix} \dot{z}_1 \\ \dot{z}_2 \end{pmatrix} = -\frac{1}{2\ell} \begin{pmatrix} v_1 & v_2 - iv_3 \\ v_2 + iv_3 & -v_1 \end{pmatrix} \begin{pmatrix} z_1 \\ z_2 \end{pmatrix}, \quad \dot{\Gamma} = (v_1, v_2, v_3), \tag{12}$$

via the complex Hopf fibration $\mathbb{C}^2 \setminus 0 \to S^2$,

$$\begin{pmatrix} z_1 \\ z_2 \end{pmatrix} \mapsto \mathbf{r} = \left(\frac{|z_1|^2 - |z_2|^2}{|z_1|^2 + |z_2|^2}, \frac{2\bar{z}_1 z_2}{|z_1|^2 + |z_2|^2} \right) \in \mathbb{R} \oplus \mathbb{C} = \mathbb{R}^3.$$

Using the complex coordinate $z = z_2/z_1 = (r_2 + ir_3)/(1 + r_1)$ on $S^2 \simeq \mathbb{CP}^1$, the linear system (12) projects to the complex Riccati equation

$$\dot{z} = \frac{1}{2\ell}\left(-q + 2v_1 z + \bar{q} z^2\right), \quad \dot{\Gamma} = \mathbf{v} = (v_1, v_2, v_3), \quad q = v_2 + iv_3. \tag{13}$$

Downloaded from https://academic.oup.com/imrn/advance-article-abstract/doi/10.1093/imrn/rny087/4998816 by Pennsylvania State University user on 15 January 2019

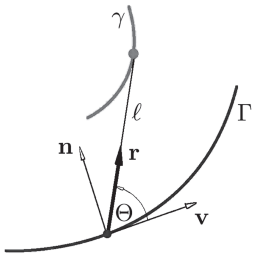

Fig. 10. The Frenet–Serret frame along Γ.

It follows that the bicycle monodromy in $\mathbb{R}^3$ is given by elements of the complex Möbius group $\mathrm{PSL}_2(\mathbb{C})$.

The proof is by direct calculation which we omit. In the next subsection we give a more conceptual (group theoretic) explanation of Theorems 1 and 2.

Remark 2.8. Note that the Riccati equation (13) reduces to (6) for $q = v_2$, that is, for a planar curve Γ with $v_3 = 0$.

We now derive a "moving-frame" version of (13). Assume Γ is parameterized by arc length, so that $\mathbf{v} = \dot{\Gamma}$ is a unit vector, and complete $\mathbf{v}$ to the Frenet–Serret frame ($\mathbf{v}$, $\mathbf{n}$, $\mathbf{b}$) along Γ, satisfying the equations

$$\dot{\mathbf{v}} = \kappa \mathbf{n}, \quad \dot{\mathbf{n}} = -\kappa \mathbf{v} + \tau \mathbf{b}, \quad \dot{\mathbf{b}} = -\tau \mathbf{n},$$

where κ, τ are the curvature and torsion of Γ. See Figure 10.

Proposition 2.9. Let $\mathbf{r} = R_1 \mathbf{v} + R_2 \mathbf{n} + R_3 \mathbf{b}$ be a unit vector field along an arc length parameterized curve Γ in $\mathbb{R}^3$. Then $\mathbf{r}(t)$ satisfies (11) if and only if $\mathbf{R} = (R_1, R_2, R_3)$ satisfies

$$\dot{\mathbf{R}} = \left[\frac{1}{\ell} \mathbf{E}_1 \times \mathbf{R} - \Omega \right] \times \mathbf{R}, \tag{14}$$

where $\Omega = \tau \mathbf{E}_1 + \kappa \mathbf{E}_3$ (the Darboux vector of Γ in the Frenet frame) and

$$\mathbf{E}_1 = \begin{pmatrix} 1 \\ 0 \\ 0 \end{pmatrix}, \quad \mathbf{E}_3 = \begin{pmatrix} 0 \\ 0 \\ 1 \end{pmatrix}.$$

Downloaded from https://academic.oup.com/imrn/advance-article-abstract/doi/10.1093/imrn/rny087/4998816 by Pennsylvania State University user on 15 January 2019

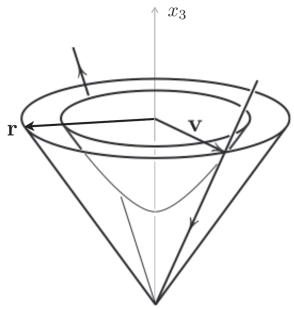

Fig. 11. The null cone in $\mathbb{R}^{2,1}$. The arrows along the two cone generators show the direction of the flow along the eigendirections of A in Lemma 2.11.

Using the complex coordinate $Z = (R_2 + iR_3)/(1 + R_1)$ on the $\mathbf{R}$-sphere (stereographic projection from $-\mathbf{E}_1$ onto the (R_2, R_3)-plane), we obtain the complex Riccati equation

$$\dot{Z} = \left(\frac{1}{\ell} - i\tau\right) Z - \frac{\kappa}{2}(1 + Z^2), \tag{15}$$

the projectivization $Z = Z_2/Z_1$ of the linear system

$$\begin{pmatrix} \dot{Z}_1 \\ \dot{Z}_2 \end{pmatrix} = \frac{1}{2} \begin{pmatrix} -1/\ell + i\tau & \kappa \\ -\kappa & 1/\ell - i\tau \end{pmatrix} \begin{pmatrix} Z_1 \\ Z_2 \end{pmatrix}. \tag{16}$$

The proof is again a direct calculation that we omit.

Note that the bracketed term in (14) is the angular velocity of the bike expressed in the Frenet frame. Note also that (15) reduces to (10) for a planar curve ($\tau = 0$).

2.5 Reformulation for general n using the Möbius group

In this section we present another way to interpret the bicycle flow (4). To illustrate the idea for $n = 2$ (the higher dimensional case works almost verbatim), the circle $\|\mathbf{r}\| = 1$ is embedded in Minkowski's three-space $\mathbb{R}^3$ as shown in Figure 11; namely, as the intersection of the cone $x_1^2 + x_2^2 - x_3^2 = 0$ and the horizontal plane $x_3 = 1$. Each generating ray of the cone is uniquely determined by a unit vector $\mathbf{r}$, as shown in Figure 11. We then consider *linear* flows in $\mathbb{R}^3$ preserving the Lorentz quadratic form $x_1^2 + x_2^2 - x_3^2$, so that the cone is invariant under any such Lorentz–orthogonal flow. We show that the bicycle flow on $\mathbf{r}$ at time t corresponds to a particular linear Lorentz–orthogonal flow, namely, to

Downloaded from https://academic.oup.com/imrn/advance-article-abstract/doi/10.1093/imrn/rny087/4998816 by Pennsylvania State University user on 15 January 2019

Downloaded from https://academic.oup.com/imrn/advance-article-abstract/doi/10.1093/imrn/rny087/4998816 by Pennsylvania State University user on 15 January 2019

a flow with two eigendirections lying in the vertical plane through the origin containing $\pm\mathbf{v}$, where $\mathbf{v} = \dot{\Gamma}(t)$.

The same construction shows how the bicycle flow extends from the circle $\|\mathbf{r}\| = 1$ to a flow of the disk $\|\mathbf{r}\| < 1$ by hyperbolic isometries.

We now proceed with the formal discussion for general n.

Let $\mathbb{R}^{n,1}$ be $n+1$–dimensional space equipped with the quadratic form

$$\langle \mathbf{x}, \mathbf{x} \rangle := (x_1)^2 + \ldots + (x_n)^2 - (x_{n+1})^2, \quad \mathbf{x} = (x_1, \ldots, x_{n+1}).$$

Let $\mathrm{SO}^+_{n,1} \subset \mathrm{GL}(\mathbb{R}^{n,1})$ be the orientation and time-orientation preserving linear isometries of $\mathbb{R}^{n,1}$ (the identity component of the Lorentz-orthogonal group $\mathrm{O}_{n,1}$). Its Lie algebra $\mathfrak{so}_{n,1}$ consists of $(n+1) \times (n+1)$ matrices, written in block form as

$$\begin{pmatrix} B & \mathbf{v} \\ \mathbf{v}^t & 0 \end{pmatrix}, \quad \mathbf{v} = (v_1, \ldots, v_n)^t \in \mathbb{R}^n, \quad B \in \mathfrak{so}_n \text{ (i.e., } B^t = -B).$$

Let

$$\mathbb{R}^{n,1}_+ = \{\mathbf{x} \in \mathbb{R}^{n,1} \mid x_{n+1} > 0\}$$

and

$$\pi : \mathbb{R}^{n,1}_+ \to \mathbb{R}^n, \quad \mathbf{x} = (x, x_{n+1}) \mapsto \frac{x}{x_{n+1}}, \quad x = (x_1, \ldots, x_n). \tag{17}$$

For each $\ell > 0$, let

$$H^n_\ell = \left\{\mathbf{x} \in \mathbb{R}^{n,1}_+ \mid \langle \mathbf{x}, \mathbf{x} \rangle = -\ell^2\right\} \tag{18}$$

and

$$\mathcal{C} = \left\{\mathbf{x} \in \mathbb{R}^{n,1}_+ \mid \langle \mathbf{x}, \mathbf{x} \rangle = 0\right\}.$$

Equip $\mathbb{R}^{n,1}$ with the flat pseudo-Riemannian metric induced by $\langle \cdot, \cdot \rangle$,

$$g = \langle d\mathbf{x}, d\mathbf{x} \rangle = (dx_1)^2 + \ldots + (dx_n)^2 - (dx_{n+1})^2.$$

Using this notation, we collect in the next proposition some standard facts about the geometry of the $\mathrm{SO}^+_{n,1}$-action on $\mathbb{R}^{n,1}$; see, for example, [8].

Proposition 2.10. For all $n \geq 2$,

1. H^n_ℓ and $\mathcal{C}$ are the $\mathrm{SO}^+_{n,1}$-orbits of $(\ell, 0, \ldots, 0)^t$ and $(1, 0, \ldots, 0, 1)^t$, respectively.

2. The flat pseudo-Riemannian metric $g = \langle \mathbf{dx}, \mathbf{dx} \rangle$ on $\mathbb{R}^{n,1}$ restricts on H^n_ℓ to a Riemannian metric of constant negative sectional curvature $-1/\ell^2$, on which $\mathrm{SO}^+_{n,1}$ acts transitively as its group of orientation preserving isometries. (H^n_1 is the "hyperboloid model" of the hyperbolic n-space.)
3. For each $\ell > 0$, the restriction of π to $H^n_\ell \subset \mathbb{R}^{n,1}_+$ is a diffeomorphism onto the unit ball $B^n = \{\mathbf{r} \in \mathbb{R}^n \mid \|\mathbf{r}\| < 1\}$. The induced metric on B^n is

$$\mathrm{d}s^2_\ell = \frac{\ell^2}{1 - \|\mathbf{r}\|^2} \left(\frac{(\mathbf{r} \cdot \mathrm{d}\mathbf{r})^2}{1 - \|\mathbf{r}\|^2} + \|\mathrm{d}\mathbf{r}\|^2 \right). \tag{19}$$

   (B^n, equipped with this metric for $\ell = 1$, is the Klein–Beltrami or projective model of hyperbolic n-space.)
4. The restriction of g to $\mathcal{C}$ is degenerate (for all $\mathbf{x} \in \mathcal{C}$ the line $\mathbb{R}\mathbf{x} \subset T_{\mathbf{x}}\mathcal{C}$ is orthogonal to $T_{\mathbf{x}}\mathcal{C}$), descending to a conformal Riemannian metric on its spherization $S^{n-1} = \mathcal{C}/\mathbb{R}^+$, isomorphic to the standard conformal structure on S^{n-1} (see next item).
5. The image of $\mathcal{C}$ under π is $S^{n-1} = \partial B^n$. The metric g, restricted to $\mathcal{C}$, descends via π to the standard ("round") conformal metric on S^{n-1}. The action of $\mathrm{SO}^+_{n,1}$ on $\mathcal{C}$ descends to S^{n-1}, preserving the conformal structure. The group $\mathrm{SO}^+_{n,1}$ acting in the described way is called the Möbius group $\mathrm{Mob}(S^{n-1})$.
6. $\mathrm{Mob}(S^n)$, for $n \geq 2$, is the full group of orientation preserving conformal transformations of S^n. $\mathrm{Mob}(S^1)$ is the projective group $\mathrm{PSL}_2(\mathbb{R})$.

The following lemma is borrowed from [35]. We reproduce its proof here for the convenience of the reader.

Lemma 2.11. For each $\mathbf{v} \in \mathbb{R}^n$, consider the linear vector field v on $\mathbb{R}^{n,1}$, $v(\mathbf{x}) = A\mathbf{x}$, where

$$A = -\begin{pmatrix} 0_n & \mathbf{v} \\ \mathbf{v}^t & 0 \end{pmatrix} \in \mathfrak{so}_{n,1}.$$

Then, under the projection $\pi : \mathbb{R}^{n,1}_+ \to \mathbb{R}^n$ of formula (17), v maps to the vector field on $\mathbb{R}^n$ defined by the right hand side of (4).

Proof. Let $\mathbf{x} = (x, x_{n+1}) \in \mathbb{R}^{n,1}_+$ and $\delta\mathbf{x} = (\delta x, \delta x_{n+1})$ a tangent vector at $\mathbf{x}$, where $x = (x_1, \ldots, x_n)$. Then, by formula (17), the derivative of π at $\mathbf{x}$ is $\delta\mathbf{x} \mapsto (x_{n+1}\delta x - x\delta x_{n+1})/(x_{n+1})^2$. Next, let $\delta\mathbf{x} = v(\mathbf{x}) = A\mathbf{x}$. Then $\delta\mathbf{x} = (\delta x, \delta x_{n+1})$, where $\delta x = -x_{n+1}\mathbf{v}$

Downloaded from https://academic.oup.com/imrn/advance-article-abstract/doi/10.1093/imrn/rny087/4998816 by Pennsylvania State University user on 15 January 2019

and $\delta x_{n+1} = -x \cdot \mathbf{v}$. It follows that the image of $v(\mathbf{x})$ under $\mathrm{d}\pi$ is

$$\frac{x_{n+1}(-x_{n+1}\mathbf{v}) - x(-x \cdot \mathbf{v})}{x_{n+1}^2} = -\mathbf{v} + (\mathbf{v} \cdot \mathbf{r})\mathbf{r}.$$

■

As a consequence of the previous proposition and lemma, we obtain the following theorem, proved for $n = 2$ in [17], and for general n in [35].

Theorem 3. The flow of equation (4) (for all $\mathbf{r}$) is the projection via $\pi : \mathbb{R}^{n,1}_{+} \to \mathbb{R}^n$ (defined in (17)) of the flow of the linear system in $\mathbb{R}^{n,1}$ with $\mathfrak{so}_{n,1}$ coefficient matrix

$$\dot{\mathbf{x}} = -\frac{1}{\ell}\begin{pmatrix} 0_n & \mathbf{v} \\ \mathbf{v}^t & 0 \end{pmatrix}\mathbf{x}, \quad \mathbf{v} = \dot{\Gamma}. \tag{20}$$

It follows that

(1) The bicycle monodromy $M^t_\ell : S^{n-1} \to S^{n-1}$ is a Möbius transformation, well-defined for all t for which $\Gamma(t)$ is defined.
(2) The flow of (4) preserves the unit open ball $B^n = \{\|\mathbf{r}\| < 1\}$, on which it acts by isometries of the hyperbolic metric of (19).

Remark 2.12. In Section 2.10 below we interpret the hyperbolic isometries of item (2) of Theorem 3 above as "rolling without slipping and twisting" of H^n_ℓ along $\Gamma \subset \mathbb{R}^n$. The flow of (4) also preserves the complement of the closed unit ball $\{\|\mathbf{r}\| > 1\}$ on which it acts by isometries of a (curved) Lorenzian metric. We do not pursue here this aspect of the bicycle monodromy, but it would be interesting to find a mechanical-geometric interpretation of this flow.

Remark 2.13. The bicycle equation (4) can be also reformulated in the language of bundles and connections, which some readers might find useful (a similar interpretation for $n = 2$ appeared in [17]). This formulation leads to a straightforward generalization of the bicycling equation on any Riemannian manifold. We sketch here this formulation.

Downloaded from https://academic.oup.com/imrn/advance-article-abstract/doi/10.1093/imrn/rny087/4998816 by Pennsylvania State University user on 15 January 2019

Consider the $\mathfrak{so}_{n,1}$-valued one-form on $\mathbb{R}^n$

$$\theta = \frac{1}{\ell}\begin{pmatrix} 0 & \cdots & 0 & \mathrm{d}x_1 \\ \vdots & \vdots & \vdots & \vdots \\ 0 & \cdots & 0 & \mathrm{d}x_n \\ \mathrm{d}x_1 & \cdots & \mathrm{d}x_n & 0 \end{pmatrix}. \tag{21}$$

We view θ as the one-form of an $\mathrm{SO}^+_{n,1}$-connection on the trivial principal bundle $\mathbb{R}^n \times \mathrm{SO}^+_{n,1} \to \mathbb{R}^n$. For any space F on which $\mathrm{SO}^+_{n,1}$ acts, θ defines the covariant derivative $\mathrm{D} = \mathrm{d} + \theta$ of sections $f : \mathbb{R}^n \to F$ of the associated bundle $\mathbb{R}^n \times F \to \mathbb{R}^n$. Namely, $\mathrm{D}f = \mathrm{d}f + \theta \cdot f$, and a section is parallel if $\mathrm{D}f = 0$.

Equation (20) is then the equation for parallel transport in the vector bundle associated to the standard representation of $\mathrm{SO}^+_{n,1}$ on $\mathbb{R}^{n,1}$. The projectivization of this representation has three orbits: the projectivized null cone S^{n-1}, its interior B^n, and the exterior $\mathbb{RP}^n \setminus \overline{B^n}$. On each of these orbits $\mathrm{SO}^+_{n,1}$ acts as the automorphism group of a different structure: isometries of a hyperbolic metric on B^n, Möbius transformation of S^{n-1}, and isometries of a Lorentzian metric on $\mathbb{RP}^n \setminus \overline{B^n}$. The parallel transport in the associated bundle $\mathbb{R}^n \times \mathbb{RP}^n \to \mathbb{R}^n$ is given by the bicycle equation (4), where $\mathbf{r}$ is used as an affine coordinate.

For an arbitrary Riemannian manifold M the ℓ-bicycling equation defines an $\mathrm{SO}^+_{n,1}$-connection on its unit tangent sphere bundle. In general, this connection is non-flat, unless M has a metric of constant curvature $-1/\ell^2$, that is, is hyperbolic, in which case the connection defines an interesting foliation of the unit tangent bundle of M. See Example 3.6.17 on p. 165 of [37].

2.6 The special isomorphisms $\mathfrak{so}_{2,1} \simeq \mathfrak{sl}_2(\mathbb{R})$, $\mathfrak{so}_{3,1} \simeq \mathfrak{sl}_2(\mathbb{C})$

For $n = 2$, 3 there are "special isomorphisms" which enable us to replace (20) with a more compact linear system with 2×2 real or complex matrices instead of 3×3 or 4×4 real matrices (respectively).

2.6.1 $n = 2$

Let $\mathfrak{sl}_2(\mathbb{R})$ be the Lie algebra of $\mathrm{SL}_2(\mathbb{R})$, that is, the set of traceless real 2×2 matrices A. We equip $\mathfrak{sl}_2(\mathbb{R})$ with the quadratic form $-\det(A)$; this form has signature (2, 1), suggesting a relation with $\mathbb{R}^{2,1}$; indeed, one has the following.

Downloaded from https://academic.oup.com/imrn/advance-article-abstract/doi/10.1093/imrn/rny087/4998816 by Pennsylvania State University user on 15 January 2019

Downloaded from https://academic.oup.com/imrn/advance-article-abstract/doi/10.1093/imrn/rny087/4998816 by Pennsylvania State University user on 15 January 2019

Proposition 2.14. The map $\mathbb{R}^{2,1} \to \mathfrak{sl}_2(\mathbb{R})$,

$$\mathbf{x} = (x_1, x_2, x_3) \mapsto A = \begin{pmatrix} -x_2 & x_1 + x_3 \\ x_1 - x_3 & x_2 \end{pmatrix},$$

is an isometry, mapping the quadratic form $\langle \mathbf{x}, \mathbf{x} \rangle = (x_1)^2 + (x_2)^2 - (x_3)^2$ to $-\det(A)$. The conjugation action of $\mathrm{SL}_2(\mathbb{R})$ on $\mathfrak{sl}_2(\mathbb{R})$, $A \mapsto gAg^{-1}$, preserves the quadratic form $-\det(A)$. The resulting homomorphism $\mathrm{SL}_2(\mathbb{R}) \to \mathrm{SO}^+_{2,1}$ is surjective with kernel $\{I, -I\}$. The corresponding isomorphism of Lie algebras $\mathfrak{sl}_2(\mathbb{R}) \simeq \mathfrak{so}_{2,1}$ is

$$\begin{pmatrix} v_1 & v_2 \\ v_3 & -v_1 \end{pmatrix} \mapsto \begin{pmatrix} 0 & v_3 - v_2 & 2v_1 \\ v_2 - v_3 & 0 & v_2 + v_3 \\ 2v_1 & v_2 + v_3 & 0 \end{pmatrix}. \tag{22}$$

Proof. A direct calculation which we omit. ■

In particular, applying the inverse of the isomorphism (22) to the coefficient matrix of the system (20) for $n = 2$,

$$-\frac{1}{\ell} \begin{pmatrix} 0 & 0 & v_1 \\ 0 & 0 & v_2 \\ v_1 & v_2 & 0 \end{pmatrix} \mapsto -\frac{1}{2\ell} \begin{pmatrix} v_1 & v_2 \\ v_2 & -v_1 \end{pmatrix},$$

we obtain the system (7) (which we obtained previously by different means):

$$\begin{pmatrix} \dot{x} \\ \dot{y} \end{pmatrix} = -\frac{1}{2\ell} \begin{pmatrix} v_1 & v_2 \\ v_2 & -v_1 \end{pmatrix} \begin{pmatrix} x \\ y \end{pmatrix}.$$

2.6.2 $n = 3$

Let $\mathcal{H}$ be the space of 2×2 complex Hermitian matrices, $A = \bar{A}^t$, equipped with the (real) quadratic form $-\det(A)$ of signature (3, 1).

Proposition 2.15. The map $\mathbb{R}^{3,1} \to \mathcal{H}$,

$$\mathbf{x} = (x_1, x_2, x_3, x_4) \mapsto A = \begin{pmatrix} -x_1 + x_4 & -x_2 + ix_3 \\ -x_2 - ix_3 & x_1 + x_4 \end{pmatrix},$$

is an isometry, mapping the quadratic form $\langle \mathbf{x}, \mathbf{x} \rangle = (x_1)^2+(x_2)^2+(x_3)^2-(x_4)^2$ to $-\det(A)$. The linear action of $\mathrm{SL}_2(\mathbb{C})$ on $\mathcal{H}$, $A \mapsto gA\bar{g}^t$, preserves the quadratic form $-\det(A)$. The resulting homomorphism $\mathrm{SL}_2(\mathbb{C}) \to \mathrm{SO}^+_{3,1}$ is surjective with kernel $\{I, -I\}$. The associated isomorphism of Lie algebras $\mathfrak{sl}_2(\mathbb{C}) \simeq \mathfrak{so}_{3,1}$ is

$$\begin{pmatrix} a & b \\ c & -a \end{pmatrix} \mapsto \begin{pmatrix} 0 & b_1 - c_1 & -b_2 - c_2 & -2a_1 \\ -b_1 + c_1 & 0 & 2a_2 & -b_1 - c_1 \\ b_2 + c_2 & -2a_2 & 0 & b_2 - c_2 \\ -2a_1 & -b_1 - c_1 & b_2 - c_2 & 0 \end{pmatrix}, \tag{23}$$

where $a = a_1 + ia_2, b = b_1 + ib_2, c = c_1 + ic_2$.

Proof. Another computation that we omit. ■

Applying the inverse of the isomorphism (23) to the coefficient matrix of the system (20) for $n = 3$,

$$-\frac{1}{\ell}\begin{pmatrix} 0 & 0 & 0 & v_1 \\ 0 & 0 & 0 & v_2 \\ 0 & 0 & 0 & v_3 \\ v_1 & v_2 & v_3 & 0 \end{pmatrix} \mapsto -\frac{1}{2\ell}\begin{pmatrix} v_1 & v_2 - iv_3 \\ v_2 + iv_3 & -v_1 \end{pmatrix},$$

we obtain the two-dimensional complex linear system

$$\begin{pmatrix} \dot{z}_1 \\ \dot{z}_2 \end{pmatrix} = -\frac{1}{2\ell}\begin{pmatrix} v_1 & v_2 - iv_3 \\ v_2 + iv_3 & -v_1 \end{pmatrix}\begin{pmatrix} z_1 \\ z_2 \end{pmatrix}, \quad \dot{\Gamma} = (v_1, v_2, v_3),$$

which we also obtained previously in (12) by different means.

Remark 2.16. Although not used in this article, two other special isomorphisms are $\mathfrak{so}_{5,1} \simeq \mathfrak{sl}_2(\mathbb{H})$ and $\mathfrak{so}_{9,1} \simeq \mathfrak{sl}_2(\mathbb{O})$ (see, e.g., [49]). Hence the bicycle equation in $\mathbb{R}^5$ and $\mathbb{R}^9$ can also be "linearized" by two-dimensional quaternionic and octonionic linear systems (respectively), with the corresponding Riccati equations. The quaternionic system is

$$\begin{pmatrix} \dot{h}_1 \\ \dot{h}_2 \end{pmatrix} = -\frac{1}{2\ell}\begin{pmatrix} v_1 & \bar{q} \\ q & -v_1 \end{pmatrix}\begin{pmatrix} h_1 \\ h_2 \end{pmatrix},$$

Downloaded from https://academic.oup.com/imrn/advance-article-abstract/doi/10.1093/imrn/rny087/4998816 by Pennsylvania State University user on 15 January 2019

Downloaded from https://academic.oup.com/imrn/advance-article-abstract/doi/10.1093/imrn/rny087/4998816 by Pennsylvania State University user on 15 January 2019

where

$$\dot{\Gamma} = (v_1, \dots, v_5), \quad q = v_2 + iv_3 + jv_4 + kv_5 \in \mathbb{H},$$

with the quaternionic Riccati equation for $h = h_2 h_1^{-1}$

$$\dot{h} = \frac{1}{2\ell}(-q + 2v_1 h + h\bar{q}h).$$

2.7 A Berry phase formula for the bicycle monodromy

Let Γ be a parameterized front curve in $\mathbb{R}^n$ and $M_\ell : S^{n-1} \to S^{n-1}$ the associated ℓ-bicycle monodromy between two points $\Gamma(t_0), \Gamma(t_1)$ on Γ, with $t_0 < t_1$.

Theorem 4. For every $n \geq 2$, $\ell > 0$, and $\mathbf{r}_0 \in S^{n-1}$, the derivative $M'_\ell(\mathbf{r}_0) : T_{\mathbf{r}_0} S^{n-1} \to T_{\mathbf{r}_1} S^{n-1}$ is given by

$$M'_\ell(\mathbf{r}_0) = e^{-L_\gamma/\ell} P,$$

where

- $\mathbf{r}_1 = \mathbf{r}(t_1)$ and $\mathbf{r}(t)$ is the solution to (4) with $\mathbf{r}(t_0) = \mathbf{r}_0$,
- $\gamma(t) = \Gamma(t) + \ell \mathbf{r}(t)$ is the corresponding rear track,
- $L_\gamma = -\int_{t_0}^{t_1} \mathbf{r} \cdot \mathbf{v}\, \mathrm{d}t$, $\mathbf{v} = \dot{\Gamma}$, is the (signed) length of γ,
- $P \in \mathrm{Iso}(T_{\mathbf{r}_0} S^{n-1}, T_{\mathbf{r}_1} S^{n-1})$ is the parallel transport in TS^{n-1} (with respect to the Levi–Civita connection) along the curve $\mathbf{r}(t)$, $t_0 \leq t \leq t_1$.

Remark 2.17. The sign of the length element $-\mathbf{r} \cdot \mathbf{v}\, \mathrm{d}t$ of the rear track is adjusted to coincide with the geometric intuition of forward riding of γ being counted as positive length and backward riding as negative. The sign is reversed at a cusp.

Proof of Theorem 4. Note first that for every $\boldsymbol{\xi}_0 \in T_{\mathbf{r}_0} S^{n-1}$, one has $M'_\ell(\mathbf{r}_0)\boldsymbol{\xi}_0 = \boldsymbol{\xi}(t_1)$, where $\boldsymbol{\xi}(t) \in T_{\mathbf{r}(t)} S^{n-1}$ is the solution to the linearization of (4) along $\mathbf{r}(t)$, satisfying $\boldsymbol{\xi}(t_0) = \boldsymbol{\xi}_0$; namely,

$$\ell \dot{\boldsymbol{\xi}} = (\mathbf{v} \cdot \boldsymbol{\xi})\mathbf{r} + (\mathbf{v} \cdot \mathbf{r})\boldsymbol{\xi}, \quad \mathbf{v} = \dot{\Gamma}.$$

It follows that $(\mathbf{v} \cdot \mathbf{r})\boldsymbol{\xi}/\ell$ is the orthogonal projection of $\dot{\boldsymbol{\xi}}$ on $T_{\mathbf{r}} S^{n-1}$. But this is precisely the definition of the covariant derivative along a submanifold in $\mathbb{R}^n$. That is,

$$\nabla_{\dot{\mathbf{r}}} \boldsymbol{\xi} = \frac{\mathbf{r} \cdot \mathbf{v}}{\ell} \boldsymbol{\xi}, \tag{24}$$

where ∇ is the Levi–Civita connection on S^{n-1}.

Next, let $u := (\mathbf{r} \cdot \mathbf{v})/\ell$, $f(t) := \exp\left(\int_{t_0}^{t} u(s)\,\mathrm{d}s\right)$ and $\hat{\boldsymbol{\xi}}(t)$ the parallel transport of $\boldsymbol{\xi}(t_0)$ along $\mathbf{r}(t)$; that is, $\hat{\boldsymbol{\xi}}(t_0) = \boldsymbol{\xi}(t_0)$, and $\nabla_{\dot{\mathbf{r}}}\hat{\boldsymbol{\xi}} = 0$. The theorem then amounts to $\boldsymbol{\xi} = f\hat{\boldsymbol{\xi}}$. To show this, it is enough to show that both $\boldsymbol{\xi}, f\hat{\boldsymbol{\xi}}$ have the same value at $t = t_0$ and satisfy the same first order differential equation. By (24), $\boldsymbol{\xi}$ satisfies $\nabla_{\dot{\mathbf{r}}}\boldsymbol{\xi} = u\boldsymbol{\xi}$. Now f, by its definition, satisfies $f(t_0) = 1$ and $\dot{f} = uf$, hence $(f\hat{\boldsymbol{\xi}})(t_0) = \boldsymbol{\xi}(t_0)$ and

$$\nabla_{\dot{\mathbf{r}}}(f\hat{\boldsymbol{\xi}}) = \dot{f}\hat{\boldsymbol{\xi}} + f\nabla_{\dot{\mathbf{r}}}\hat{\boldsymbol{\xi}} = \dot{f}\hat{\boldsymbol{\xi}} = u(f\hat{\boldsymbol{\xi}}).$$

Therefore $\boldsymbol{\xi} = f\hat{\boldsymbol{\xi}}$. ■

Remark 2.18. For $n \geq 3$, Theorem 4 implies that M_ℓ is a conformal transformation (since parallel transport is an isometry), so it gives an alternative proof of Theorem 3, item 1.

The most interesting case of Theorem 4 is that of a closed curve in $\mathbb{R}^3$, where $M_\ell \in \mathrm{PSL}_2(\mathbb{C})$. Generically, M_ℓ has two fixed points in S^2 and is thus conjugate to the Möbius transformation $z \mapsto \lambda z$, whose fixed points are $0, \infty$, with $M'(0) = \lambda, M'(\infty) = 1/\lambda$. The *conjugacy class* of M is thus given by the derivatives $\lambda^{\pm 1}$ at the fixed points.

Corollary 2.19. (Berry phase formula) Let Γ be a closed curve in $\mathbb{R}^3$, $\mathbf{r}_0 \in S^2$ a fixed point of the ℓ-bicycle monodromy of Γ (with respect to some initial point $\Gamma(t_0)$), and γ the corresponding closed rear track. Then

$$M'_\ell(\mathbf{r}_0) = e^{-(L_\gamma/\ell)+i\Omega}, \tag{25}$$

where L_γ is the signed length of γ and Ω is the area in S^2 enclosed by the spherical curve $\mathbf{r}(t)$.

Proof. By the Gauss–Bonnet theorem, parallel transport around a closed curve in S^2 is a rotation by an angle equal to the area of the spherical region bounded by the curve. ■

Remark 2.20.

(i) The last corollary and its proof still hold when the spherical curve $\mathbf{r}(t)$ is not simple, provided Ω is defined as the algebraic (or signed) area of the spherical region bounded by $\mathbf{r}(t)$; see, for example, [2].

Downloaded from https://academic.oup.com/imrn/advance-article-abstract/doi/10.1093/imrn/rny087/4998816 by Pennsylvania State University user on 15 January 2019

(ii) For $n = 2$, in the case of hyperbolic monodromy, with γ being one of the two periodic rear tracks, the formula reduces to $M'_\ell(\mathbf{r}_0) = e^{-L_\gamma/\ell}$, as in Theorem 3.6 of [35]. This formula determines the conjugacy class of the bicycle monodromy when it is a hyperbolic element of $\mathrm{PSL}_2(\mathbb{R})$. The elliptic case, on the other hand, becomes clear only once we embed the bike in $\mathbb{R}^3$, as explained below in Section 2.9.

(iii) For a generic Γ in $\mathbb{R}^3$, the M_ℓ–iterates of all points on the sphere, except for the unstable fixed point, approach the stable fixed point. This means that all spatial motions of the bike, save the unstable periodic one, approach the stable periodic motion. The case of planar Γ (in $\mathbb{R}^3$) is special: M_ℓ commutes with reflections in the plane, and in the elliptic case M is conjugate to a rigid rotation of S^2. All the bike motions in $\mathbb{R}^3$ are then periodic or quasiperiodic with two frequencies.

(iv) In the planar elliptic case embedded in $\mathbb{R}^3$, the length of each of the two periodic rear tracks is zero, as follows from (25).

(v) Here is a heuristic explanation for the appearance of Berry phase Ω in formula (25). Figure 12 shows two infinitesimally close bikes, with rear wheels at R, R_1, sharing the same front trajectory Γ at F, with R tracing a closed back track γ and R_1 a nearby (not necessarily closed) back track. Consider the unit vector $\hat{\boldsymbol{\xi}} = RR_1/|RR_1|$. The key observation is that *the angular velocity of $\hat{\boldsymbol{\xi}}$ around the axis RF is zero.*

To justify this, let us decompose $\mathbf{v} = \dot{F}$ as $\mathbf{v} = \mathbf{v}_{plane} + \mathbf{v}^\perp$, where $\mathbf{v}_{plane}$ is the orthogonal projection of $\mathbf{v}$ unto the FRR_1–plane and $\mathbf{v}^\perp$ the perpendicular component, as shown in Figure 12. Let us consider separately the effects of $\mathbf{v}_{plane}$ and $\mathbf{v}^\perp$.

First, the motion of R and R_1 due to $\mathbf{v}_{plane}$ occurs in the plane RFR_1, and thus $\hat{\boldsymbol{\xi}} \parallel RR_1$ does not rotate about any axis in that plane, let alone about FR. Second, the component $\mathbf{v}^\perp$ does not even contribute to the velocities of R and R_1, and therefore $\mathbf{v}^\perp$ has no effect on the motion of $\hat{\boldsymbol{\xi}}$.

This zero angular velocity statement is equivalent to saying that $\hat{\boldsymbol{\xi}}$ *undergoes parallel transport on the sphere centered at F along the curve traced on it by R*. It follows, by the Gauss–Bonnet theorem, that the vector $\hat{\boldsymbol{\xi}}$ will end up rotated by an angle, equal to the solid angle Ω (or spherical area) bounded by the closed path traced by R, as viewed by an observer moving with F.

Downloaded from https://academic.oup.com/imrn/advance-article-abstract/doi/10.1093/imrn/rny087/4998816 by Pennsylvania State University user on 15 January 2019

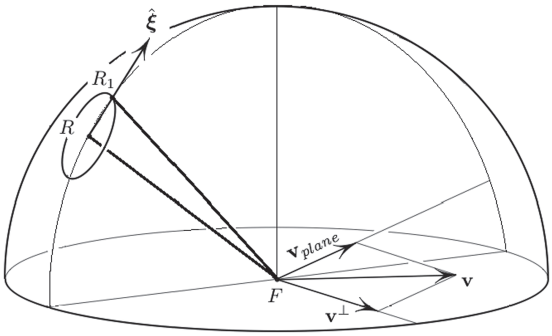

Fig. 12. A heuristic explanation for the appearance of Berry's phase.

2.8 Bicycle as a planimeter in $\mathbb{R}^n$

As we mentioned in the introduction, the planar bicycle can serve as a planimeter. In this section, we examine the higher dimensional version of this phenomenon.

Let Γ be a closed curve in $\mathbb{R}^n$, the bicycle front track, of length L. Let the bicycle length be $\ell = 1/\varepsilon$; as before, $\mathbf{v} = \dot{\Gamma}$ and $\mathbf{r}$ is a unit vector along the bicycle segment. The bicycle equation (4) with an initial condition is

$$\begin{cases} \dot{\mathbf{r}} = \varepsilon(-\mathbf{v} + (\mathbf{v}\cdot\mathbf{r})\mathbf{r}), \\ \mathbf{r}(0,\varepsilon) = \mathbf{r}_0. \end{cases} \tag{26}$$

The following theorem generalizes the hatchet planimeter formula (1). The area bounded by a closed plane curve $\Gamma(t)$ is given by the integral

$$\frac{1}{2}\int \det(\Gamma, \dot{\Gamma})\, \mathrm{d}t.$$

For a curve Γ in $\mathbb{R}^n$, an analog of the area is the area bivector

$$\frac{1}{2}\int \Gamma \wedge \dot{\Gamma}\, \mathrm{d}t,$$

which contains the information about the areas bounded by the projections of the curve on all coordinate two-planes, see Remark 2.22 below. This bivector can be interpreted as a skew–symmetric linear operator.

Downloaded from https://academic.oup.com/imrn/advance-article-abstract/doi/10.1093/imrn/rny087/4998816 by Pennsylvania State University user on 15 January 2019

Downloaded from https://academic.oup.com/imrn/advance-article-abstract/doi/10.1093/imrn/rny087/4998816 by Pennsylvania State University user on 15 January 2019

Theorem 5. The bicycle vector $\mathbf{r}$, that is, the solution of (26), undergoes a net rigid rotation, up to an $O(\varepsilon^3)$–error; more precisely,

$$\mathbf{r}(L) = \mathbf{r}_0 + \varepsilon^2 \mathcal{A}\mathbf{r}_0 + O(\varepsilon^3), \tag{27}$$

where $\mathcal{A} : \mathbb{R}^n \to \mathbb{R}^n$ is the skew–symmetric "area operator" of Γ, given by

$$\mathcal{A}\mathbf{r}_0 = \int_0^L (\Gamma \cdot \mathbf{r}_0)\dot{\Gamma}\, \mathrm{d}t, \quad \text{for} \quad \mathbf{r}_0 \in \mathbb{R}^n.$$

For $n = 3$,

$$\mathcal{A}\mathbf{r}_0 = \int_0^L (\Gamma \cdot \mathbf{r}_0)\dot{\Gamma}\, \mathrm{d}t = \widehat{\mathcal{A}} \times \mathbf{r}_0, \tag{28}$$

where

$$\widehat{\mathcal{A}} = \frac{1}{2}\int_0^L (\Gamma \times \dot{\Gamma})\, \mathrm{d}t$$

is the area vector of Γ. Thus in $\mathbb{R}^3$, modulo an $O(\varepsilon^3)$–error, the initial bike direction $\mathbf{r}_0$ is rotated around the direction $\widehat{\mathcal{A}}$ through the angle $\|\widehat{\mathcal{A}}\|$, equal to the signed area of the projection of Γ on a plane perpendicular to $\widehat{\mathcal{A}}$.

Proof. The solution $\mathbf{r}(t, \varepsilon)$ of the Cauchy problem (26) is analytic in ε since so is the right-hand side, and thus can be expanded in a Taylor series in ε, starting with

$$\mathbf{r}(t, \varepsilon) = \mathbf{r}(t, 0) + \mathbf{r}_1(t)\varepsilon + \mathbf{r}_2(t)\varepsilon^2 + O(\varepsilon^3), \tag{29}$$

where $\mathbf{r}_1(t) = \partial_\varepsilon \mathbf{r}(t, 0)$, $\mathbf{r}_2(t) = \frac{1}{2}\partial_\varepsilon^2 \mathbf{r}(t, 0)$. To find $\mathbf{r}(t, 0), \mathbf{r}_1(t), \mathbf{r}_2(t)$, we first set $\varepsilon = 0$ in (26) to find $\mathbf{r}(t, 0) \equiv \mathbf{r}_0$. Differentiating (26) by ε two times and setting $\varepsilon = 0$ after each differentiation, we get

$$\dot{\mathbf{r}}_1 = -\mathbf{v} + (\mathbf{v} \cdot \mathbf{r}_0)\mathbf{r}_0 \tag{30}$$

and

$$\dot{\mathbf{r}}_2 = (\mathbf{v} \cdot \mathbf{r}_1)\mathbf{r}_0 + (\mathbf{v} \cdot \mathbf{r}_0)\mathbf{r}_1. \tag{31}$$

From (30),

$$\mathbf{r}_1 = -\Gamma + (\Gamma \cdot \mathbf{r}_0)\mathbf{r}_0 + \mathbf{c}, \tag{32}$$

and in particular $\mathbf{r}_1(L) = \mathbf{r}_1(0)$. Substituting (32) into (31) and integrating, we find, after simplification, the sole surviving term (other terms drop out as the derivatives

of periodic functions):

$$\mathbf{r}_2\Big|_{t=0}^{L} = -\int_0^L (\dot{\Gamma}\cdot\mathbf{r}_0)\Gamma\,\mathrm{d}t = \int_0^L (\Gamma\cdot\mathbf{r}_0)\dot{\Gamma}\,\mathrm{d}t,$$

the last step using integration by parts.

For $n=3$, integrating the identity

$$(\Gamma\times\dot{\Gamma})\times\mathbf{r}_0 = (\mathbf{r}_0\cdot\Gamma)\dot{\Gamma} - (\mathbf{r}_0\cdot\dot{\Gamma})\Gamma$$

over a period and using integration by parts, one obtains the stated formula. ■

Remark 2.21. Theorem 5 reveals an interesting behavior of the bicycle equation in $\mathbb{R}^3$ for large bike length. On the one hand, the bicycle vector field on S^2 given by (26) is "maximally hyperbolic", in the sense that the two instantaneous equilibria at $\mathbf{r}=\pm\mathbf{v}/\|\mathbf{v}\|$ are antipodal nodes on the $\mathbf{r}$-sphere, one stable (at $-\mathbf{v}/\|\mathbf{v}\|$), the other unstable (at $\mathbf{v}/\|\mathbf{v}\|$). On the other hand, the time L map $\mathbf{r}_0\mapsto\mathbf{r}(L)$ of this vector field, that is, the monodromy map, is "maximally elliptic" in the sense that it is $O(\varepsilon^3)$–close to a rigid rotation, with antipodal pair of elliptic fixed points.

Remark 2.22. The entries $\mathcal{A}_{ij}=-\mathcal{A}_{ji}$ are the signed areas of the projections of Γ onto the ijth planes, so $\mathcal{A}$ is the area bivector of the curve Γ. For $n=2$,

$$\mathcal{A} = \begin{pmatrix} 0 & -A_\Gamma \\ A_\Gamma & 0 \end{pmatrix},$$

where A_Γ is the signed area of Γ, reproducing the planimeter formula (1).

Remark 2.23. The classical literature on the hatchet planimeter contains a series, in the negative powers of the length of the planimeter ℓ, of its turning angle θ, see, for example, [26]. This makes it possible to estimate the error in measuring the area effectively. It should be possible to obtain a similar power expansion in the multi-dimensional setting; we do not dwell on it here.

2.9 A bird's eye view of the hatchet planimeter

The results of the last two subsections lead to a new intuitive understanding of the hatchet planimeter formula (1), which we describe in this subsection. Loosely speaking,

Downloaded from https://academic.oup.com/imrn/advance-article-abstract/doi/10.1093/imrn/rny087/4998816 by Pennsylvania State University user on 15 January 2019

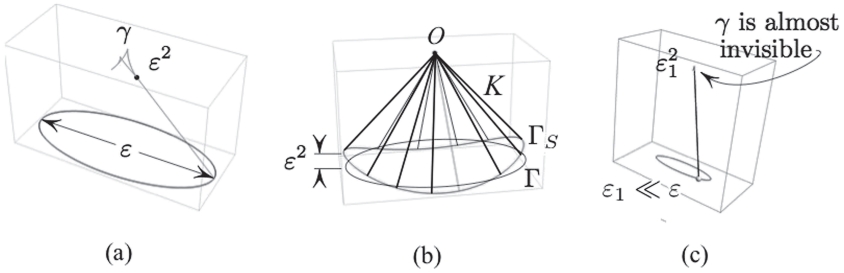

Fig. 13. (a) $\mathrm{diam}(\Gamma) = O(\varepsilon)$, $\mathrm{diam}(\gamma) = O(\varepsilon^2)$. (b) Γ is $O(\varepsilon^2)$–close to Γ_S. (c) As ε decreases to $\varepsilon_1 \ll \varepsilon$, γ becomes indistinguishable from a point, and thus Γ_S looks indistinguishable from Γ, illustrating (34).

the angle by which the planimeter rotates is approximated by the solid angle of a certain cone, as explained next.

We consider a planar curve $\Gamma \subset \mathbb{R}^2$ of small diameter $\mathrm{diam}(\Gamma) = O(\varepsilon)$, area $A = O(\varepsilon^2)$, and fixed bicycle length $\ell = 1$—this assumption is equivalent to taking a long bike of size $\ell = 1/\varepsilon$ for a fixed Γ.

With Γ so scaled, the hatchet planimeter formula (1), expressing the area A bounded by Γ in terms of the rotation angle θ of the planimeter, becomes

$$A = \theta + O(\varepsilon^3). \tag{33}$$

We now "lift" our point of view above Γ by considering the plane $\mathbb{R}^2$ containing Γ as the horizonal plane $z = 0$ in $\mathbb{R}^3$. The monodromy of Γ then becomes a Möbius transformation $M : S^2 \to S^2$, commuting with the reflection about the horizontal plane and conjugate to a rigid rotation about a vertical axis, with a pair of fixed points, symmetrically situated on opposite sides of the horizontal equator $S^1 \subset S^2$. Consider the closed rear track γ corresponding to one of those fixed point; see Figure 13(a).

Let us parallel transport every bike segment RF tangent to γ by moving the tangency point R to a chosen point $O \in \gamma$. The translated segments form a cone K with vertex at O and the translated endpoints F form a curve Γ_S on the unit sphere S^2 centered at O, enclosing a spherical area Ω, equal to the solid angle subtended by K at O; see Figure 13(b).

The Berry's phase formula (Corollary 2.19) states that M (the monodromy of Γ) is conjugate to a rigid rotation of S^2 by the angle Ω (note that $L_\gamma = 0$ in (25) for a planar Γ with an elliptic M). Furthermore, Theorem 5 states that M is $O(\varepsilon^3)$–close to a rigid

Downloaded from https://academic.oup.com/imrn/advance-article-abstract/doi/10.1093/imrn/rny087/4998816 by Pennsylvania State University user on 15 January 2019

rotation. Combining the last two statements, we conclude that the rotation angle θ of the planimeter in formula (33) is $O(\varepsilon^3)$–close to the solid angle Ω. In other words, formula (33) is equivalent to the statement

$$A = \Omega + O(\varepsilon^3). \tag{34}$$

Formula (34) suggests a "bird's eye view" interpretation of the planimeter formula (33): a bird standing at a point O, at height 1 above a planar curve Γ of diameter $O(\varepsilon)$, estimates its area A, with $O(\varepsilon^3)$–accuracy, by the solid angle Ω subtended at O by the $O(\varepsilon^2)$–close curve Γ_S.

To justify the $O(\varepsilon^2)$–closeness of Γ and Γ_S, we argue as follows. First, we observe that $\operatorname{diam}(\gamma) = O(\varepsilon^2)$ as Figure 13(a) illustrates; indeed, the tangent segments RF to γ form angles $\pi/2 + O(\varepsilon)$ with the plane of Γ, and thus

$$\dot\gamma = (\mathbf{v}\cdot\mathbf{r})\mathbf{r} = \|\mathbf{v}\|\cos(\pi/2 + O(\varepsilon)) = O(\varepsilon^2),$$

since $\|\mathbf{v}\| = \|\dot\Gamma\| = O(\varepsilon)$. When constructing Γ_S we therefore moved each point $F \in \Gamma$ by $O(\varepsilon^2)$, which shows that Γ_S and Γ are $O(\varepsilon^2)$–close to each other.

This now implies (34) as follows: first, projecting Γ_S onto the horizontal plane, the area of the resulting planar region is $O(\varepsilon^3)$–close to the spherical area Ω enclosed by Γ_S; since the projected curve is $O(\varepsilon^2)$–close to Γ, and both have length $O(\varepsilon)$, their areas differ by $O(\varepsilon^3)$. This explains (34).

2.10 Bicycling and hyperbolic rolling

The main purpose of this section is to elaborate on the equivalence mentioned before (Remark 2.12): the bicycle equation (4), for $\|\mathbf{r}\| < 1$, also describes the rolling without sliding and twisting of the hyperbolic n-ball on the Euclidean n-space $\mathbb{R}^n$. A precise statement is given in Theorem 6 below. We precede this statement by a discussion of rolling of the Euclidean sphere.

We feel that this material is not common knowledge and not easy to gather from the literature, so we begin with an elementary exposition of rolling a ball on the plane, before moving on to the rolling of hyperbolic n-space on $\mathbb{R}^n$. For a more abstract "intrinsic" treatment of rolling we recommend [10] (section 4.4), as well as [9]. For $n = 2$, the material here is closely related to the "stargazing" interpretation of the bicycling (4) as it appears in Section 3 of [18].

Downloaded from https://academic.oup.com/imrn/advance-article-abstract/doi/10.1093/imrn/rny087/4998816 by Pennsylvania State University user on 15 January 2019

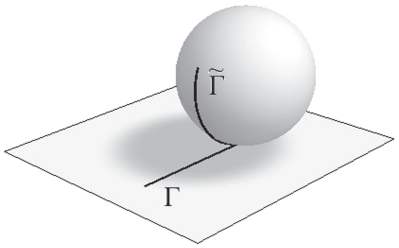

Fig. 14. A ball rolling without slipping and twisting.

Consider a rubber ball lying on top of the flat rough surface of a table, so that the ball can roll on the table, but not slide; that is, as the ball moves, at each moment the point of the ball in contact with the table has zero velocity. We paint a straight line segment Γ on the table, position the ball at one end of Γ, and roll it along until it reaches the other end. As we do so, the paint, which is still wet, marks a curve $\tilde{\Gamma}$ on the surface of the ball. See Figure 14.

Since we are rolling without sliding, $\tilde{\Gamma}$ and Γ have the same length. Furthermore, if we are careful not to spin the ball about the vertical axis through its contact point with the table as it rolls, $\tilde{\Gamma}$ is in fact a geodesic segment (an arc of a great circle). Note also that as a result of the rolling, the ball is translated along Γ and rotated about the horizontal axis passing through the center of the ball and perpendicular to the direction of Γ. Note also that due to the no-spin condition, a parallel field of vectors along Γ leaves a "track" of corresponding vectors on $\tilde{\Gamma}$ which form a parallel field with respect to parallel transport on the sphere.

We can of course roll the ball along a more general curve Γ drawn on the table, in which case the no-slide and no-spin conditions (also called "no-slip" and "no-twist") imply that the curve $\tilde{\Gamma}$ traced on the ball has the same length and the same geodesic curvature as Γ at the corresponding points. The change of orientation of the ball as a result of the rolling is an element $g \in \mathrm{SO}_3$, called the *rolling monodromy* of Γ.

For example, if Γ is a circle of radius R, then $\tilde{\Gamma}$ is an arc of a circle of latitude on the sphere, of length $2\pi R$ and geodesic curvature $1/R$, from which one can easily determine $\tilde{\Gamma}$, as well as g (given the radius of the rolling ball).

Let us now formulate the above more precisely and generally. Consider the n-sphere of radius ℓ,

$$S^n_\ell = \{(x_1, \ldots, x_{n+1}) \in \mathbb{R}^{n+1} | (x_1)^2 + \ldots + (x_{n+1})^2 = \ell^2\},$$

Downloaded from https://academic.oup.com/imrn/advance-article-abstract/doi/10.1093/imrn/rny087/4998816 by Pennsylvania State University user on 15 January 2019

rolling along a smoothly parametrized curve $\Gamma(t)$ in $\mathbb{R}^n = \{x_{n+1} = 0\} \subset \mathbb{R}^{n+1}$. The rolling motion is given by a time-dependent family of rigid motions $\varphi(t) : \mathbb{R}^{n+1} \to \mathbb{R}^{n+1}$, so that $\varphi(t)(S^n_\ell)$ is positioned in the upper half space $\{x_{n+1} \geq 0\}$, tangent to $\mathbb{R}^n$ at $\Gamma(t)$. Then $\varphi(t)$ can be written as

$$\varphi(t)(\mathbf{x}) = g(t)\mathbf{x} + \Gamma(t) + \ell e_{n+1}, \quad g(0) = \mathrm{I},$$

where $g(t) \in \mathrm{SO}_{n+1} = \mathrm{Iso}^+(S^n_\ell)$ is the "rolling monodromy", describing the rotation of the moving sphere at time t with respect to its initial position at $t = 0$. Let

$$\tilde{\Gamma}(t) = \varphi(t)^{-1}(\Gamma(t)) = -\ell[g(t)]^{-1}e_{n+1} \in S^n_\ell,$$

the "body" curve of contact points. The (space) derivative of $\varphi(t)$ is a linear isometry $T_{\tilde{\Gamma}(t)}S^n_\ell \to T_{\Gamma(t)}\mathbb{R}^n$, given by $g(t)$, satisfying the following two rolling conditions:

(1) No-slip: $g(t)\dot{\tilde{\Gamma}}(t) = \dot{\Gamma}(t)$;
(2) No-twist: if $\tilde{\boldsymbol{\xi}}$ is a vector field tangent to S^n_ℓ and parallel along $\tilde{\Gamma}$, then $g(t)\tilde{\boldsymbol{\xi}}(t)$ is parallel along Γ.

Remark 2.24. It can be easily shown that the no-slip condition (1) is equivalent to the vanishing of the Killing field $v(t) := \dot{\varphi}(t)[\varphi(t)]^{-1}$ at $\Gamma(t)$ ("the velocity of the contact point of the rolling body with $\mathbb{R}^n$ is equal to zero"). Thus, for $n = 2$, $v(t)$ is the velocity vector field of rotations about an instantaneous axis passing through the contact point $\Gamma(t)$ (the "angular velocity" axis). Furthermore, for $n = 2$, the no-twist condition (2) is equivalent to the instantaneous rotation axis lying in $\mathbb{R}^2$ and perpendicular to $\dot{\Gamma}$. It is also equivalent to the equality of the geodesic curvatures of Γ and $\tilde{\Gamma}$ at the corresponding points.

Proposition 2.25. The monodromy $g(t) \in \mathrm{SO}_{n+1}$ of rolling S^n_ℓ along a parametrized curve $\Gamma(t)$ in $\mathbb{R}^n$ satisfies

$$\dot{g} = \frac{1}{\ell}\begin{pmatrix} 0_n & \mathbf{v} \\ -\mathbf{v}^t & 0 \end{pmatrix} g, \quad g(0) = \mathrm{I}, \quad \mathbf{v} = \dot{\Gamma}. \tag{35}$$

Proof. For the sake of brevity we omit the explicit t-dependence, writing $g = g(t)$, etc.

Downloaded from https://academic.oup.com/imrn/advance-article-abstract/doi/10.1093/imrn/rny087/4998816 by Pennsylvania State University user on 15 January 2019

Downloaded from https://academic.oup.com/imrn/advance-article-abstract/doi/10.1093/imrn/rny087/4998816 by Pennsylvania State University user on 15 January 2019

Let $A = \dot{g}g^{-1} \in \mathfrak{so}_{n+1}$. The statement is then that the no-slip and no-twist conditions are equivalent to (1): $Ae_{n+1} = \dot{\Gamma}/\ell$ and (2): if $\boldsymbol{\xi} \perp e_{n+1}$ then $A\boldsymbol{\xi} \equiv 0 \pmod{e_{n+1}}$ (i.e., $A\boldsymbol{\xi}$ is a multiple of e_{n+1}). We now prove (1) and (2).

(1) $g\tilde{\Gamma} = -\ell e_{n+1}$ implies $0 = \dot{g}\tilde{\Gamma} + g\dot{\tilde{\Gamma}} = -\ell Ae_{n+1} + g\dot{\tilde{\Gamma}}$. Hence the no-slip condition, $g\dot{\tilde{\Gamma}} = \dot{\Gamma}$, is equivalent to $Ae_{n+1} = \dot{\Gamma}/\ell$.

(2) Suppose $\tilde{\boldsymbol{\xi}}$ is parallel along $\tilde{\Gamma}$. Then $\dot{\tilde{\boldsymbol{\xi}}} \equiv 0 \pmod{\tilde{\Gamma}}$, hence $g\dot{\tilde{\boldsymbol{\xi}}} \equiv 0 \pmod{e_{n+1}}$. Let $\boldsymbol{\xi} = g\tilde{\boldsymbol{\xi}}$. Then

$$\dot{\boldsymbol{\xi}} = \dot{g}\tilde{\boldsymbol{\xi}} + g\dot{\tilde{\boldsymbol{\xi}}} = A\boldsymbol{\xi} + g\dot{\tilde{\boldsymbol{\xi}}} \equiv A\boldsymbol{\xi} \pmod{e_{n+1}}.$$

But $\boldsymbol{\xi} \perp e_{n+1}$, hence $\dot{\boldsymbol{\xi}} \perp e_{n+1}$ and $\dot{\boldsymbol{\xi}} = A\boldsymbol{\xi}$. It follows that if A has the form given in formula (35), then $A\boldsymbol{\xi} = 0$, hence $\dot{\boldsymbol{\xi}} = 0$, that is, $\boldsymbol{\xi}$ is parallel.

Conversely, given a vector $\boldsymbol{\xi}_0 \perp e_{n+1}$ tangent to $\mathbb{R}^n$ at $\Gamma(t_0)$, we let $\tilde{\boldsymbol{\xi}}_0 = [g(t_0)]^{-1}\boldsymbol{\xi}_0$ and extend it to a parallel vector field $\tilde{\boldsymbol{\xi}}$ along $\tilde{\Gamma}$. Assuming the no-twist condition, $\boldsymbol{\xi} := g\tilde{\boldsymbol{\xi}}$ is parallel. As before, it implies that $0 = \dot{\boldsymbol{\xi}} \equiv A\boldsymbol{\xi} \pmod{e_{n+1}}$. In particular, $A(t_0)\boldsymbol{\xi}_0 \equiv 0 \pmod{e_{n+1}}$, as claimed. ■

Next, recall from Section 2.5 the hyperboloid model for hyperbolic n-space of curvature $-1/\ell^2$,

$$H^n_\ell = \{\mathbf{x} \in \mathbb{R}^{n,1} | \langle \mathbf{x}, \mathbf{x} \rangle = -\ell^2, x_{n+1} > 0\}.$$

Given a curve Γ in $\mathbb{R}^n = \{x_{n+1} = 0\} \subset \mathbb{R}^{n,1}$, a rolling of H^n_ℓ along Γ consists of a t-dependent family of rigid motions $\varphi(t) : \mathbb{R}^{n,1} \to \mathbb{R}^{n,1}$ (orientation preserving isometries), so that $\varphi(t)(H^n_\ell)$ is positioned in the upper half space $\{x_{n+1} \geq 0\}$, tangent to $\mathbb{R}^n$ at $\Gamma(t)$. Such $\varphi(t)$ can be written as

$$\varphi(t)(\mathbf{x}) = g(t)\mathbf{x} + \Gamma(t) - \ell e_{n+1}, \quad g(0) = \mathrm{I},$$

where $g(t) \in \mathrm{SO}^+_{n,1} = \mathrm{Iso}^+(H^n_\ell)$ is the "rolling monodromy", describing the rotation of the moving hyperbolic n-space at time t with respect to its initial position at $t = 0$. Furthermore, $g(t)$ is required to satisfy the same no-slip and no-twist conditions that were given in the case of rolling S^n_ℓ.

Theorem 6. The monodromy $g(t) \in \mathrm{SO}_{n,1}$ of rolling H^n_ℓ along a parametrized curve $\Gamma(t)$ in $\mathbb{R}^n$ satisfies

$$\dot{g} = -\frac{1}{\ell}\begin{pmatrix} 0_n & \mathbf{v} \\ \mathbf{v}^t & 0 \end{pmatrix} g, \quad g(0) = \mathrm{I}, \quad \mathbf{v} = \dot{\Gamma}. \tag{36}$$

Thus, $g(t)$ coincides with the bicycling ℓ-monodromy of Γ (see Theorem 3).

The proof is almost identical to the above proof of Proposition 2.25 and is omitted.

Remark 2.26. Embedding $\mathbb{R}^n$ and H^n_ℓ in $\mathbb{R}^{n,1}$ facilitates intuition and calculations but is not essential, since the no-slip and no-twist conditions are intrinsic. These conditions thus apply to the rolling of H^n_ℓ along an arbitrary Riemannian n-manifold M, defining a principal $\mathrm{SO}_{n,1}$-connection on M, whose associated parallel transport can be interpreted as either the monodromy of rolling H^n_ℓ along M or the monodromy of ℓ-bicycling on M.

3 Bicycle Correspondence, the Filament Equation, and Integrable Systems

3.1 Bicycle correspondence

We start by recalling the definition of the bicycle correspondence.

Definition 3.1. Let $\ell > 0$. Two smoothly parameterized curves Γ_1, Γ_2 in $\mathbb{R}^n$ are in ℓ-bicycle correspondence if, for all t,

(i) the connecting segment $\Gamma_1(t)\Gamma_2(t)$ has a fixed length ℓ, and
(ii) the midpoint curve $(\Gamma_1(t) + \Gamma_2(t))/2$ is tangent to the connecting segment.

See Figure 3 of the Introduction. Condition (ii) can be expressed by the following formula:

$$(\Gamma_1(t) - \Gamma_2(t)) \wedge (\dot\Gamma_1(t) + \dot\Gamma_2(t)) = 0. \tag{37}$$

Here is a useful reformulation. See Figure 15.

Lemma 3.2. Two parameterized curves Γ_1, Γ_2 in $\mathbb{R}^n$ are in bicycle correspondence (for some ℓ) if and only if, for all t, the vector $\dot\Gamma_2(t)$ is the reflection of $\dot\Gamma_1(t)$ about the connecting line segment $\Gamma_1(t)\Gamma_2(t)$, followed by parallel translation from $\Gamma_1(t)$ to $\Gamma_2(t)$,

$$\dot\Gamma_2(t) = -\dot\Gamma_1(t) + 2\left(\dot\Gamma_1(t)\cdot \mathbf{r}(t)\right)\mathbf{r}(t), \quad \text{where } \mathbf{r}(t) = \frac{\Gamma_1(t) - \Gamma_2(t)}{\|\Gamma_1(t) - \Gamma_2(t)\|}. \tag{38}$$

Proof. Condition (i) of Definition 3.1 is equivalent to the equality of the orthogonal projections of $\dot\Gamma_1(t)$ and $\dot\Gamma_2(t)$ onto $\mathbf{r}(t)$. Condition (ii), by formula (37), is then that the orthogonal components sum up to 0. ■

Downloaded from https://academic.oup.com/imrn/advance-article-abstract/doi/10.1093/imrn/rny087/4998816 by Pennsylvania State University user on 15 January 2019

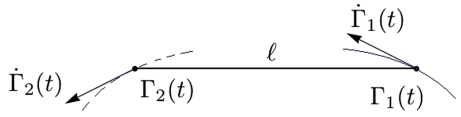

Fig. 15. ℓ-bicycle correspondence.

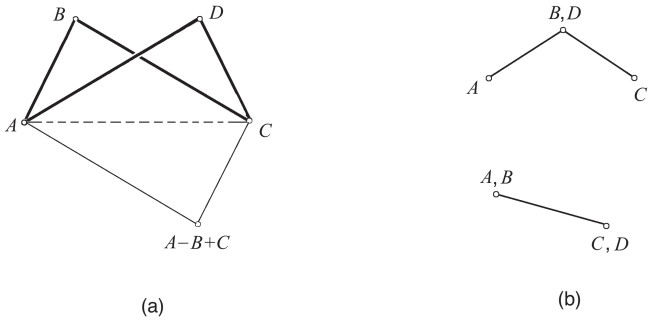

Fig. 16. (a) The definition of a Darboux Butterfly; (b) Degenerate butterflies.

Corollary 3.3. Bicycle correspondence is arc-length preserving.

Proof. This follows from Lemma 3.2 and the fact that reflection and parallel translation are isometries. ■

The main result of this section is that bicycle correspondence preserves the bicycle monodromy (Theorem 7). This result is not new: in [47], it is established for the discrete version of the bicycle correspondence, defined for polygons in $\mathbb{R}^n$, and in the smooth case, it follows by taking limit. Here we give a different proof whose idea is to conjugate the bicycle monodromies along the corresponding curves using "Darboux Butterflies", which we now introduce.

Definition 3.4. A Darboux Butterfly in $\mathbb{R}^n$ is the result of "folding" a parallelogram about one of its diagonals; more precisely, it is an ordered quadruple $ABCD$ of four distinct points in $\mathbb{R}^n$, such that D is the reflection of the point $A-B+C$ about the line AC. See Figure 16.

Remark 3.5. The above definition applies also to "degenerate" butterflies $ABCD$, where one or two pairs of points coincide, as long as $A \neq C$ or $B \neq D$, so one can apply the definition, or the equivalent one: A is the reflection of $B - C + D$ about BD.

Downloaded from https://academic.oup.com/imrn/advance-article-abstract/doi/10.1093/imrn/rny087/4998816 by Pennsylvania State University user on 15 January 2019

Here are some immediate consequences of Definition 3.4:

Lemma 3.6.

(i) A Darboux Butterfly is a planar quadrilateral.

(ii) The butterfly property is invariant under cyclic permutation and order reversing of its vertices. Namely, if $ABCD$ is a Darboux Butterfly, then so are $BCDA$ and $DCBA$.

(iii) Any triple of points ABC in $\mathbb{R}^n$ with $A \neq C$ can be completed uniquely to a Darboux Butterfly $ABCD$ (possibly degenerate; see Remark 3.5).

Another property of Darboux Butterflies is the following infinitesimal version of the "Butterfly Lemma" of [47]. To formulate it, we first define for a given segment UV in $\mathbb{R}^n$ the *glide reflection* $G_{UV} : \mathbb{R}^n \to \mathbb{R}^n$ as the composition of the reflection about the line through UV, followed by parallel translation through the vector $V - U$. For example, in Figure 15, $\dot{\Gamma}_2(t)$ is the image of $\dot{\Gamma}_1(t)$ under $G_{\Gamma_1(t)\Gamma_2(t)}$.

Lemma 3.7. For any Darboux Butterfly $ABCD$, one has

$$G_{DA} \circ G_{CD} \circ G_{BC} \circ G_{AB} = Id.$$

Proof. The linear part of the isometry in question is the composition of four reflections. Decompose $\mathbb{R}^n$ into the direct sum of the plane of the butterfly, translated to the origin, and its orthogonal complement. In the orthogonal complement each reflection acts by -1, hence the composition of the four reflections acts trivially.

In the plane of the butterfly, the product of the reflections about two successive edges is a rotation by twice the angle between the edges; the product of reflections about the next pair of successive edges is then a rotation by the same angle in opposite direction.

It follows that the linear part of the isometry in question is trivial. Thus it is a parallel translation. But A is a fixed point, hence it is the identity. ■

The next statement is a version of "Bianchi permutability" [40], proved in [47] for a polygonal version of the bicycle correspondence.

Proposition 3.8. Let $\ell_1, \ell_2 > 0$ with $\ell_1 \neq \ell_2$ and let $A(t)$, $B(t)$, $C(t)$ be three parameterized curves in $\mathbb{R}^n$ such that (A, B) and (B, C) are in ℓ_1- and ℓ_2-bicycle correspondences, respec-

Downloaded from https://academic.oup.com/imrn/advance-article-abstract/doi/10.1093/imrn/rny087/4998816 by Pennsylvania State University user on 15 January 2019

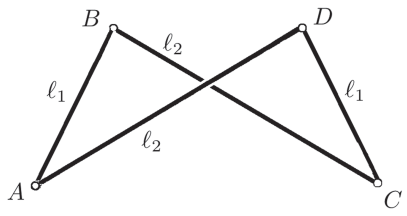

Fig. 17. Bianchi permutability.

tively. Complete $A(t)B(t)C(t)$ to a Darboux Butterfly $A(t)B(t)C(t)D(t)$ (the non-degeneracy assumption $\ell_1 \neq \ell_2$ assures that $A(t) \neq C(t)$ so Lemma 3.6(iii) applies). Then (A, D) and (C, D) are in ℓ_2- and ℓ_1-bicycle correspondence, respectively. See Figure 17.

Proof. By Lemma 3.2, $\dot{A} = G_{BA}\dot{B}, \dot{C} = G_{BC}\dot{B}$, and we need to show that $\dot{D} = G_{AD}\dot{A} = G_{CD}\dot{C}$.

Now $\|A - D\| = \ell_2$ and $\|C - D\| = \ell_1$ imply the "non-stretching condition": the orthogonal projections of $\dot{D}$ onto AD and CD coincide with the orthogonal projections of $\dot{A}$ and $\dot{C}$ onto AD and CD, respectively. If the butterfly is noncollinear then AD, CD are linearly independent, hence $\dot{D}$ is determined uniquely by the non-stretching condition. On the other hand, using Lemma 3.7, we have

$$G_{AD}\dot{A} = G_{AD}G_{BA}\dot{B} = G_{CD}G_{BC}\dot{B} = G_{CD}\dot{C},$$

and this vector clearly satisfies the "non-stretching condition". Hence $\dot{D} = G_{AD}\dot{A} = G_{CD}\dot{C}$. For a collinear butterfly, the result follows by continuity from the noncollinear case. ■

The next result shows that the flows of the bicycle equation along curves in bicycle correspondence are conjugate.

Lemma 3.9. Let Γ_1, Γ_2 be two parameterized curves in $\mathbb{R}^n$ in 2ℓ-bicycle correspondence. For each $\lambda \neq \ell$, let $\Phi^\lambda(t) : S^{n-1} \to S^{n-1}$ be the map $\mathbf{r}_1 \mapsto \mathbf{r}_2$ defined by completing $\Gamma_1(t) + 2\lambda\mathbf{r}_1, \Gamma_1(t), \Gamma_2(t)$ to a Darboux Butterfly

$$\Gamma_1(t) + 2\lambda\mathbf{r}_1, \Gamma_1(t), \Gamma_2(t), \Gamma_2(t) + 2\lambda\mathbf{r}_2$$

Downloaded from https://academic.oup.com/imrn/advance-article-abstract/doi/10.1093/imrn/rny087/4998816 by Pennsylvania State University user on 15 January 2019

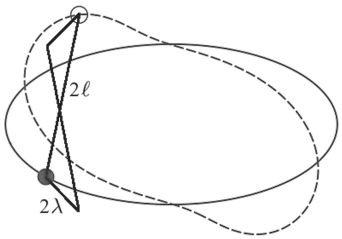

Fig. 18. Two closed curves in 2ℓ-bicycle correspondence, with the Darboux Butterfly conjugating their λ-bicycle flows.

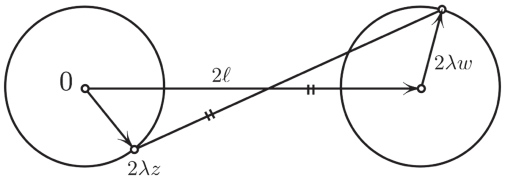

Fig. 19.. Proving that Φ^λ is a Möbius transformation.

(see Figure 18). Then $\Phi^\lambda(t)$ is a Möbius transformation (possibly orientation reversing), conjugating the λ-bicycle flows along Γ_1, Γ_2. That is, if $\mathbf{r}_1(t)$ satisfies $\lambda\dot{\mathbf{r}}_1 = -\mathbf{v}_1 + (\mathbf{v}_1 \cdot \mathbf{r}_1)\mathbf{r}_1$ then $\mathbf{r}_2(t) := \Phi^\lambda(t)\mathbf{r}_1(t)$ satisfies $\lambda\dot{\mathbf{r}}_2 = -\mathbf{v}_2 + (\mathbf{v}_2 \cdot \mathbf{r}_2)\mathbf{r}_2$, where $\mathbf{v}_1 = \dot{\Gamma}_1, \mathbf{v}_2 = \dot{\Gamma}_2$.

Proof. If $\mathbf{r}_1(t)$ solves the λ-bicycle equation along Γ_1 then $\Gamma_1 + 2\lambda\mathbf{r}_1$ is in 2λ-bicycle correspondence with Γ_1. By Bianchi permutability (Proposition 3.8), $\Gamma_2 + 2\lambda\mathbf{r}_2$ is in 2λ-bicycle correspondence with Γ_2, hence $\mathbf{r}_2(t)$ is a solution to the λ-bicycle equation along Γ_2.

The proof that $\Phi^\lambda(t)$ is a Möbius transformation was given in the proof of Theorem 1 of [47]. Here we present an alternative proof for $n = 2$, that is, $\Phi^\lambda(t) : S^1 \to S^1$, where $S^1 \subset \mathbb{C}$. We denote the image of z by w, where $|z| = |w| = 1$, see Figure 19. Expanding $|2\ell + 2\lambda w - 2\lambda z|^2 = (2\ell)^2$, we obtain

$$\mathrm{Re}\Big(w(\lambda\bar{z} - \ell) + (\ell\bar{z} - \lambda)\Big) = 0. \tag{39}$$

Geometrically, it is clear that given any $z \neq \pm 1$ on the unit circle, there are precisely two solutions w to (39), and that one of them is $w = z$ (corresponding to the parallelogram, rather than the butterfly). The other (algebraically) obvious solution is

Downloaded from https://academic.oup.com/imrn/advance-article-abstract/doi/10.1093/imrn/rny087/4998816 by Pennsylvania State University user on 15 January 2019

Downloaded from https://academic.oup.com/imrn/advance-article-abstract/doi/10.1093/imrn/rny087/4998816 by Pennsylvania State University user on 15 January 2019

given simply by

$$w(\lambda\bar{z}-\ell)+(\ell\bar{z}-\lambda)=0,$$

or

$$w=-\frac{\ell\bar{z}-\lambda}{\lambda\bar{z}-\ell}.$$

The last formula shows that $z\mapsto w$ is a reflection $z\mapsto\bar{z}$, followed by a Möbius transformation, the projectivization of $\begin{pmatrix}\ell & -\lambda\\ -\lambda & \ell\end{pmatrix}\in \mathrm{GL}_2(\mathbb{R})$, as claimed. ■

Theorem 7. If Γ_1,Γ_2 are two closed curves in $\mathbb{R}^n$ in 2ℓ-bicycle correspondence then, for all $\lambda>0$, their λ-bicycle monodromies are conjugate elements of $\mathrm{SO}^+_{n,1}$.

Proof. For $\lambda\neq\ell$ this follows from the last lemma. By continuity, it then follows also for $\lambda=\ell$. ■

This theorem provides integrals of the bicycle correspondence: a conjugacy-invariant function on the Möbius group, considered as a function of λ, is such an integral. Individual integrals can be obtained by expanding such a function in a series in λ. We call such integrals of the bicycle correspondence the monodromy integrals.

For a discussion of symplectic properties and complete integrability of the bicycle correspondence, see [48].

3.2 The bicycle equation and the filament equation

In this subsection we describe a relation between the bicycle equation (4) in $\mathbb{R}^3$ and the *filament equation* (also called the *localized induction equation*, among several other names). The later is an evolution equation on arc length parameterized curves $\Gamma(t)$ in $\mathbb{R}^3$,

$$\Gamma'=\dot{\Gamma}\times\ddot{\Gamma},$$

where prime $'$ denotes time derivative and dot stands for derivative with respect to arc length t along Γ (this unconventional choice is forced by the prior role of t in this paper). In other words, the point $\Gamma(t)$ moves in the binormal direction with velocity equal to the curvature $\kappa(t)$. This equation provides a simplified model of the motion of a vortex line in ideal fluid. Here we are concerned with closed curves.

This infinite-dimensional system is completely integrable in the following sense (see [29, 30]). It is a Hamiltonian system with respect to the so-called Marsden–

Weinstein symplectic structure on the space of arc length parameterized curves, the Hamiltonian function being the perimeter of the curve. We do not use this symplectic structure in the present paper, so we simply refer to [39] and [3], p. 326 and p. 332, for its definition and main properties.

The filament equation has a hierarchy of Poisson commuting integrals $F_1, F_2, \dots$ that starts with

$$\int 1 \, \mathrm{d}t, \ \int \tau \, \mathrm{d}t, \ \int \kappa^2 \, \mathrm{d}t, \ \int \kappa^2 \tau \, \mathrm{d}t, \int \left(\dot{\kappa}^2 + \kappa^2 \tau^2 - \frac{1}{4} \kappa^4 \right) \mathrm{d}t, \dots, \tag{40}$$

where, as before, τ is the torsion and κ is the curvature of Γ. One also has a hierarchy of vector fields $\mathbf{x}_0, \mathbf{x}_1, \mathbf{x}_2, \dots$ along Γ, that starts with

$$-\mathbf{v}, \ \kappa \mathbf{b}, \frac{\kappa^2}{2} \mathbf{v} + \dot{\kappa} \mathbf{n} + \kappa \tau \mathbf{b}, \ \kappa^2 \tau \mathbf{v} + (2 \dot{\kappa} \tau + \kappa \dot{\tau}) \mathbf{n} + \left(\kappa \tau^2 - \ddot{\kappa} - \frac{\kappa^3}{2} \right) \mathbf{b}, \dots, \tag{41}$$

where, as before, $\mathbf{v}$, $\mathbf{n}$, $\mathbf{b}$ is the Frenet frame along Γ. For each $i \geq 1$, $\mathbf{x}_i$ defines a Hamiltonian vector field on the space of arc length parameterized curves in $\mathbb{R}^3$, whose Hamiltonian with respect to the Marsden–Weinstein structure is F_i.

The vector fields $\mathbf{x}_i$ satisfy the relations

$$\dot{\mathbf{x}}_i = \mathbf{v} \times \mathbf{x}_{i+1}, \quad i = 0, 1, 2, \dots. \tag{42}$$

Following [29], [19], consider the generating function $\mathbf{x} := \sum_{j \geq 0} \varepsilon^j \mathbf{x}_j$, where ε is a formal parameter. Then the relations (42) can be compactly encoded in the equation

$$\varepsilon \dot{\mathbf{x}} = \mathbf{v} \times \mathbf{x}, \quad \mathbf{v} = \dot{\Gamma}. \tag{43}$$

We impose an additional normalization condition $\mathbf{x} \cdot \mathbf{x} = 1$; the vector fields $\mathbf{x}_i$ are then uniquely defined by (43) and $\mathbf{x}_0 = -\mathbf{v}$ (see [29]).

Remark 3.10. The series $\mathbf{x} = \sum_{j \geq 0} \varepsilon^j \mathbf{x}_j$ is a formal periodic solution of the differential equation (43) on the sphere. We do not claim that it converges and represents a genuine periodic solution for any $\varepsilon \neq 0$.

Now let us compare (43) with the bicycle equation (11) in $\mathbb{R}^3$:

$$\ell \dot{\mathbf{r}} = (\mathbf{v} \times \mathbf{r}) \times \mathbf{r}, \quad \mathbf{r} \cdot \mathbf{r} = 1, \quad \mathbf{v} = \dot{\Gamma}. \tag{44}$$

Downloaded from https://academic.oup.com/imrn/advance-article-abstract/doi/10.1093/imrn/rny087/4998816 by Pennsylvania State University user on 15 January 2019

Downloaded from https://academic.oup.com/imrn/advance-article-abstract/doi/10.1093/imrn/rny087/4998816 by Pennsylvania State University user on 15 January 2019

Each of the right hand sides of the last two displayed equations defines a time-dependent vector field on S^2, determined by $\mathbf{v}(t) = \dot{\Gamma}(t)$. For equation (43), it is the velocity field of rotations about the axis $\mathbb{R}\mathbf{v}$ with angular velocity $\|\mathbf{v}\|$.

Proposition 3.11. The vector field on the right hand side of (43) is obtained from that on the right-hand side of (44) by an anti-clockwise rotation by 90 degrees.

The proof is straightforward from the equations.

Consequently, if we use a stereographic projection to put a complex coordinate on S^2, the resulting Riccati equations (in an inertial frame) differ by multiplication of their right-hand sides by i:

$$\ell \dot{z} = \frac{1}{2}\left(-q + 2v_1 z + \bar{q}z^2\right), \qquad \text{(Bicycle)}$$

$$\varepsilon \dot{w} = \frac{i}{2}\left(-q + 2v_1 w + \bar{q}w^2\right), \qquad \text{(Filament)}$$

where

$$\dot{\Gamma} = \mathbf{v} = (v_1, v_2, v_3), \quad q = v_2 + iv_3.$$

In other words, the filament equation (43) is the equation of a bicycle with "imaginary length" $\ell = -i\varepsilon$.

We also have a filament analog of Proposition 2.9: we project the curve $\mathbf{x}(t)$ stereographically from $-\mathbf{v}$ (the south pole in Figure 20) on the $\mathbf{n}$, $\mathbf{b}$ plane, equipped with complex coordinate $W = (X_2 + iX_3)/(1 + X_1)$, where $\mathbf{x} = X_1\mathbf{v} + X_2\mathbf{n} + X_3\mathbf{b}$, and express (43) as a differential equation on W.

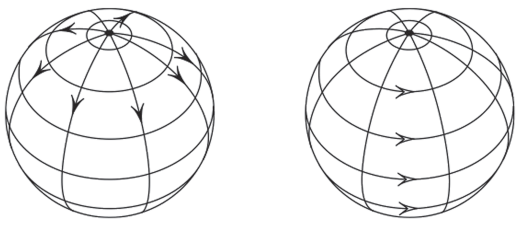

Fig. 20. The vector field of the filament equation (43) (right) is obtained from that of the bicycle equation (44) (left) by a 90° anticlockwise rotation; the fixed points ("north" and "south poles") of both vector fields are in the direction of $\pm\mathbf{v}$.

Proposition 3.12. Equation (43) is equivalent to the Riccati equation

$$\dot{W} = i\left(\frac{1}{\varepsilon} - \tau\right) W - \frac{\kappa}{2}(1 + W^2). \tag{45}$$

The proof is a direct calculation that we do not reproduce here.

Remark 3.13. Equation (43) is a particular case of the equation $\dot{\mathbf{x}} = \Omega(t)\mathbf{x}$, where Ω is a time-dependent skew-symmetric 3×3 matrix, studied in [32]. Its monodromy is the orthogonal transformation that relates the initial and terminal unit tangent vectors of the spherical curve $\mathbf{b}(t)$ whose geodesic curvature, in our case, equals

$$\frac{\tau(t) + \frac{1}{\varepsilon}}{\kappa(t)}.$$

Comparing the filament Riccati equation (45) to the bicycle Ricatti equation (15)

$$\dot{Z} = \left(\frac{1}{\ell} - i\tau\right) Z - \frac{\kappa}{2}(1 + Z^2), \tag{46}$$

we see that they are almost the same.

Corollary 3.14. The filament Riccati equation (45) is obtained from the bicycle Ricatti equation (46) by replacing the variable Z with W and ℓ with $-i\varepsilon$.

We now come to the main point of this section. Let us describe first the idea before proceeding to the technical details. Let us fix a closed smooth curve Γ in $\mathbb{R}^3$. The last corollary suggests a relation between the filament integrals F_i of equation (40) and the bicycle equation (44). It is natural to seek this relation by looking at the conjugacy class of the bicycle monodromy $M_\ell \in \mathrm{PSL}_2(\mathbb{C})$. The latter has (generically) two fixed points in S^2, one stable and one unstable, and the derivative at one of them determines the conjugacy class of M_ℓ (the derivatives are the reciprocal of each other and each is the square of the corresponding eigenvalue of a matrix in $\mathrm{SL}_2(\mathbb{C})$ representing M_ℓ). We denote by $\lambda(\ell)$, for ℓ small enough, the derivative of M_ℓ at the unstable fixed point. We will show that $\ell \ln \lambda(\ell)$ has a Taylor series at $\ell = 0$, that is, is infinitely differentiable (we do not claim analyticity). The Taylor coefficients of $\ell \ln \lambda(\ell)$ at 0 are the *monodromy integrals* of Γ. They share with F_i the property of being invariant under bicycle correspondence. By linearizing the Riccati bicycle equation (46) around the unstable periodic solution, we are able to express the monodromy integrals, like the

Downloaded from https://academic.oup.com/imrn/advance-article-abstract/doi/10.1093/imrn/rny087/4998816 by Pennsylvania State University user on 15 January 2019

Downloaded from https://academic.oup.com/imrn/advance-article-abstract/doi/10.1093/imrn/rny087/4998816 by Pennsylvania State University user on 15 January 2019

filament invariants F_i, as integrals along Γ of certain differential polynomials in κ, τ. We can then check that the first few monodromy integrals coincide with the filament invariants F_i, up to index shift and multiplicative constants. This suggests a conjectured relation between the filament integrals and the monodromy invariants.

The following proposition is the main technical tool for implementing the above plan.

Proposition 3.15. Consider a closed smooth curve Γ in $\mathbb{R}^3$. Then there exists $\ell_0 > 0$ such that for all $\ell \in (0, \ell_0)$ the associated Ricatti equation (46) has a unique unstable periodic solution $Z(t, \ell)$, tending uniformly, with all its derivatives, to the zero function, as $\ell \to 0$. Furthermore, extended to $\ell = 0$ via $Z(t, 0) = 0$, $Z(t, \ell)$ is infinitely differentiable in $\mathbb{R} \times [0, \ell_0)$.

We defer the proof of this proposition to Appendix B.

Theorem 8. Let Γ be a closed smooth curve in $\mathbb{R}^3$ and denote by $\lambda(\ell) \in \mathbb{C}$ the derivative of the ℓ-bicycle monodromy at its unstable fixed point, for small enough ℓ (as per Proposition 3.15). Then $\ell \ln \lambda(\ell)$ extends to an infinitely differentiable function in $[0, \ell_0)$ for some $\ell_0 > 0$. The Taylor coefficients at 0, that is, the numbers

$$I_n := \frac{1}{n!}(\partial_\ell)^n\big|_{\ell=0}\left[\ell \ln \lambda(\ell)\right], \quad n \geq 0,$$

are invariants of the bicycle correspondence and can be determined recursively as integrals along Γ of polynomials in κ, τ and their derivatives.

Proof. We linearize (46) at the unstable periodic solution $Z(t, \ell)$, writing this linearization in the form

$$\frac{\dot{U}}{U} = \frac{1}{\ell} - i\tau - \kappa Z.$$

Integrating both sides over a period and multiplying the result by ℓ give

$$\ell \ln \lambda(\ell) = \int (1 - i\ell\tau - \ell\kappa Z)\, \mathrm{d}t. \tag{47}$$

By Proposition 3.15, this expression is C^∞ in $[0, \ell_0)$ for some $\ell_0 > 0$. To compute the derivatives of the last equation with respect to ℓ at $\ell = 0$, we need to calculate the derivatives

$$Z_n := \frac{1}{n!}\,(\partial_\ell)^n\big|_{\ell=0} Z, \quad n \geq 0.$$

To find Z_n, we first multiply the bicycle Riccati (46) by ℓ, obtaining

$$\ell\dot{Z} = Z - \ell f, \quad \text{where } f = i\tau Z + \frac{\kappa}{2}(1+Z^2), \tag{48}$$

then differentiate n times at $\ell = 0$ (an operation justified by Proposition 3.15), obtaining, after some manipulation, the recursion relation

$$Z_n = \dot{Z}_{n-1} + \frac{1}{(n-1)!}\,\partial_\ell^{n-1}\Big|_{\ell=0} f.$$

Equivalently, and perhaps easier for calculations, one expands Z as a formal power series in ℓ

$$Z = Z_0 + \ell Z_1 + \ell^2 Z_2 + \dots$$

substitutes in (48), and equates the terms having the same degree in ℓ.

In this way, one consecutively finds

$$Z_0 = 0,\ Z_1 = \frac{\kappa}{2},\ Z_2 = \frac{\dot{\kappa}}{2} + i\frac{\tau\kappa}{2},\ Z_3 = \left(\frac{\ddot{\kappa}}{2} + \frac{\kappa^3}{8} - \frac{\tau^2\kappa}{2}\right) + i\left(\frac{\dot{\tau}\kappa}{2} + \tau\dot{\kappa}\right), \dots$$

and so on, and then

$$\begin{aligned} &I_0 = \int 1\ \mathrm{d}t,\ I_1 = -i\int \tau\ \mathrm{d}t,\ I_2 = -\frac{1}{2}\int \kappa^2\ \mathrm{d}t,\ I_3 = -\frac{i}{2}\int \kappa^2\tau\ \mathrm{d}t, \\ &I_4 = -\int\left(\frac{\kappa\ddot{\kappa}}{2} - \frac{\kappa^2\tau^2}{2} + \frac{\kappa^4}{8}\right)\mathrm{d}t, \dots \end{aligned} \tag{49}$$

and so on. ■

We make two observations:

1. The integrals I_n are real for even n and imaginary for odd n.
2. Up to multiplicative constants and index shift, the integrals (49) coincide with the integrals (40) of the filament equation.

We will not attempt to justify these observations formally here and leave their validity as conjectures, to be studied in future work.

Downloaded from https://academic.oup.com/imrn/advance-article-abstract/doi/10.1093/imrn/rny087/4998816 by Pennsylvania State University user on 15 January 2019

Downloaded from https://academic.oup.com/imrn/advance-article-abstract/doi/10.1093/imrn/rny087/4998816 by Pennsylvania State University user on 15 January 2019

Remark 3.16. One can easily verify these observations by explicit calculation for the first several cases. For example, we can see immediately from formulas (40) and (49) that

$$I_0 = F_1,\ I_1 = -iF_2,\ I_2 = -\frac{1}{2}F_3,\ I_3 = -\frac{i}{2}F_4.$$

As for I_4, we make use of the presence of total derivatives,

$$I_4 - \frac{1}{2}F_5 = -\frac{1}{2}\int \left(\kappa\ddot{\kappa} + \dot{\kappa}^2\right)\mathrm{d}t = -\frac{1}{2}\int \frac{\mathrm{d}\,(\kappa\dot{\kappa})}{\mathrm{d}t}\mathrm{d}t = 0,$$

concluding that $I_4 = \frac{1}{2}F_5$. We have tested in a similar fashion observations 1 and 2 for at least ten additional terms.

A heuristic argument for observation 1 is as follows: Corollary 3.14 suggests a Laurent expansion $\ell \ln \lambda(\ell) = \sum I_n \ell^n$ in the *complex* ℓ-plane. For imaginary ℓ, that is, $\ell = -i\varepsilon$, the monodromy is an orthogonal transformation (since the linear system (43) has antisymmetric coefficient matrix), hence $\ln \lambda$ is imaginary and $\ell \ln \lambda(\ell) = \sum (-i)^n I_n \varepsilon^k$ is real. Thus I_n is real for even n, imaginary for odd n.

Remark 3.17. That the bicycle correspondence preserves the integrals (40) of the filament equation is proved in [48].

3.3 Wegner's curves, buckled rings, and solitons of the planar filament equation

In this section we show that the Zindler curves constructed by Wegner in [50]–[55] are buckled rings. The latter are also solitons of the planar filament equation (specified later in this section), see [29].

As we mentioned in the introduction, a (planar) Bernoulli elastica is an extremum of the total squared curvature (bending energy) among curves of fixed length. That is, if $\Gamma(t)$ is an arc length parameterized curve with curvature $\kappa(t)$, one is looking for extrema of $\int_\Gamma \kappa^2(t)\,\mathrm{d}t$, subject to the constraint that the perimeter is fixed. The extremal curves satisfy the Euler–Lagrange equation

$$\ddot{\kappa} + \frac{1}{2}\kappa^3 + \lambda\kappa = 0,$$

where λ is a Lagrange multiplier; see, for example, [44].

A buckled ring is an extremum of the total squared curvature functional, subject to two constraints: both the perimeter and the area are being fixed. Buckled rings have been extensively studied, starting with Lévy [36], Halphen [24], and Greenhill [20] in the

19th century; see [1, 14] for recent works. The area constraint gives rise to a second Lagrange multiplier, μ, in the Euler–Lagrange equation of a buckled ring:

$$\ddot{\kappa} + \frac{1}{2}\kappa^3 + \lambda\kappa = \mu. \tag{50}$$

Let us turn attention to Wegner's curves, which come in two flavors, the linear (non-closed) and the circular (closed) ones. The linear curves are the curves whose curvature is proportional to the distance to the x-axis. They are the graphs $y = f(x)$, in Cartesian coordinates, where f satisfies the differential equation

$$\frac{1}{\sqrt{1+f_x^2}} = af^2 + b \tag{51}$$

with parameters a, b. The circular curves are the curves whose curvature is proportional to the distance to the origin, and are given by the graphs $r = r(\psi)$, in polar coordinates, satisfying the differential equation

$$\frac{1}{\sqrt{r^2 + r_\psi^2}} = ar^2 + b + \frac{c}{r^2} \tag{52}$$

with parameters a, b, c.

Theorem 9. Wegner's curves are buckled rings: (50) holds for the linear Wegner curves with $\lambda = 2ab, \mu = 0$, and for the circular Wegner curves with $\lambda = 8ac - 2b^2, \mu = 8a$.

Proof. Consider the linear case first. Let $x(t)$, $y(t)$ be an arc length parameterization of this curve, $\theta(t)$ be its direction, and $\kappa(t)$ its curvature. Then

$$\dot{x} = \cos\theta,\ \dot{y} = \sin\theta,\ \dot{\theta} = \kappa. \tag{53}$$

The left hand side of (51) is $\dot{x}$, and we rewrite this equation as

$$\dot{x} = ay^2 + b. \tag{54}$$

We claim that $\kappa = -2ay$. Indeed, differentiate the first equation of (53) and (54),

$$-\dot{\theta}\sin\theta = \ddot{x} = 2ay\dot{y},$$

Downloaded from https://academic.oup.com/imrn/advance-article-abstract/doi/10.1093/imrn/rny087/4998816 by Pennsylvania State University user on 15 January 2019

and use the second and third equations of (53),

$$-\kappa \sin\theta = 2ay \sin\theta,$$

implying the claim.

Now using $\kappa = -2ay$, (53) and (54), we find that

$$\ddot{\kappa} + \frac{1}{2}\kappa^3 = 4a^2 y(ay^2 + b) - 4a^3 y^3 = 4a^2 by = -2ab\kappa,$$

as needed.

The argument in the circular case is similar. Let $r(t), \psi(t)$ be the polar coordinates of the curve in an arc length parameterization and $\alpha = \theta - \psi$ the angle between the tangent to the curve and the radial direction. Then

$$\dot{r} = \cos\alpha, \quad r\dot{\psi} = \sin\alpha, \quad \dot{\theta} = \kappa = \dot{\psi} + \dot{\alpha}. \tag{55}$$

The left hand side of (52) is $\dot{\psi}$, hence we can rewrite this equation as

$$\dot{\psi} = ar^2 + b + \frac{c}{r^2}. \tag{56}$$

We claim that $\kappa = 4ar^2 + 2b$. Indeed, from (55) and (56), we get

$$\sin\alpha = r\dot{\psi} = ar^3 + br + \frac{c}{r},$$

hence

$$(\kappa - \dot{\psi})\dot{r} = \dot{\alpha}\cos\alpha = (\sin\alpha)^{\cdot} = \dot{r}\left(3ar^2 + b - \frac{c}{r^2}\right).$$

Thus

$$\kappa = \dot{\psi} + 3ar^2 + b - \frac{c}{r^2} = \left(ar^2 + b + \frac{c}{r^2}\right) + 3ar^2 + b - \frac{c}{r^2} = 4ar^2 + 2b,$$

as claimed.

Now using $\kappa = 4ar^2 + 2b$, (55), and (56), we find

$$\ddot{\kappa} + \frac{1}{2}\kappa^3 = 8a[1 - \kappa(ar^4 + br^2 + c)] + \frac{1}{2}(4ar^2 + 2b)^3 =$$
$$= 4(2a + b^3 - 4abc) + 8a(b^2 - 4ac)r^2 = 2(b^2 - 4ac)\kappa + 8a,$$

as needed. ■

Downloaded from https://academic.oup.com/imrn/advance-article-abstract/doi/10.1093/imrn/rny087/4998816 by Pennsylvania State University user on 15 January 2019

Downloaded from https://academic.oup.com/imrn/advance-article-abstract/doi/10.1093/imrn/rny087/4998816 by Pennsylvania State University user on 15 January 2019

It is known that buckled rings are solitons of the planar filament equation. Let us review this material.

Let $\Gamma(t)$ be a smooth planar arc length parameterized curve, $(\mathbf{v}, \mathbf{n})$ its Frenet frame and κ its curvature. The planar filament equation is the evolution equation

$$\Gamma' = \frac{\kappa^2}{2}\mathbf{v} + \dot{\kappa}\mathbf{n},$$

obtained from the vector field $\mathbf{x}_2$ in the filament hierarchy (41) by restricting to planar curves with $\tau = 0$. The planar filament equation has infinitely many integrals of motion, namely, the odd-numbered ones in the sequence (40), restricting again to $\tau = 0$, see [31]. The planar filament equation is equivalent to the modified Korteweg–de Vries equation, in the same way as the filament equation is equivalent to the nonlinear Schrödinger equation [31].

By solitons of the planar filament equation we mean the curves that evolve under this flow by isometries and a parameter shift. The next proposition is not new (see, e.g., [29]); we include its proof here for completeness.

Proposition 3.18. The buckled rings are solitons of the planar filament equation.

Proof. A planar curve evolves by isometries if and only if its curvature remains unchanged. Let $\Gamma(t)$ be an arc length parameterized planar curve and $\boldsymbol{\delta}(t)$ a vector field along Γ, defining its variation. Denote by κ' the directional derivative of κ with respect to $\boldsymbol{\delta}$. The change in κ due to parameter shift is $\dot{\kappa} := \frac{\mathrm{d}\kappa}{\mathrm{d}t}$. It follows that the soliton condition, requiring Γ to evolve under $\boldsymbol{\delta}$ by isometries and parameter shift, is equivalent to the condition that κ satisfies the equation $\kappa' + \lambda\dot{\kappa} = 0$ for some real constant λ.

Now a straightforward calculation shows that, for a general Γ and $\boldsymbol{\delta}$,

$$\kappa' = \ddot{\boldsymbol{\delta}} \cdot \mathbf{n} - 2\kappa\, \dot{\boldsymbol{\delta}} \cdot \mathbf{v}. \tag{57}$$

(Sketch: calculate $\ddot{\boldsymbol{\delta}} = \ddot{\Gamma}' \equiv (2u'\kappa + \kappa')\mathbf{n} \pmod{\mathbf{v}}$, where $u = |\dot{\Gamma}|$, so that $\dot{\Gamma} = u\mathbf{v}$. It follows that $\ddot{\boldsymbol{\delta}} \cdot \mathbf{n} = 2u'\kappa + \kappa'$. Next, calculate $\dot{\boldsymbol{\delta}} = \dot{\Gamma}' \equiv u'\mathbf{v} \pmod{\mathbf{n}}$, hence $u' = \dot{\boldsymbol{\delta}} \cdot \mathbf{v}$, from which (57) follows.)

In our case, $\boldsymbol{\delta} = \frac{\kappa^2}{2}\mathbf{v} + \dot{\kappa}\mathbf{n}$, which implies, again by a straightforward calculation, that

$$\ddot{\boldsymbol{\delta}} \cdot \mathbf{n} = \frac{\mathrm{d}}{\mathrm{d}t}\left(\ddot{\kappa} + \frac{1}{2}\kappa^3\right), \ \dot{\boldsymbol{\delta}} \cdot \mathbf{v} = 0.$$

Downloaded from https://academic.oup.com/imrn/advance-article-abstract/doi/10.1093/imrn/rny087/4998816 by Pennsylvania State University user on 15 January 2019

(The last equation means that the flow defined by δ on the space of parametrized curves is arc length preserving.)

It follows from the last two displayed equations that the soliton condition on Γ for the planar filament equation is

$$\kappa' + \lambda\dot{\kappa} = \frac{\mathrm{d}}{\mathrm{d}t}\left(\ddot{\kappa} + \frac{1}{2}\kappa^3 + \lambda\kappa\right) = 0,$$

or

$$\ddot{\kappa} + \frac{1}{2}\kappa^3 + \lambda\kappa = \mu,$$

that is, the Euler–Lagrange equation (50). ■

We conclude that Wegner's curves are solitons of the planar filament equation.

4 Case Study: Multiple Circles

In this section we study some interesting and nontrivial curves in bicycle correspondence with a circle.

4.1 Definition of the curves $\Gamma_{k,n}$

Denote by nS^1 the n-fold circle, parameterized by $t \mapsto e^{it} \in \mathbb{C}$, $0 \le t \le 2\pi n$. Recall that the monodromy of a closed parametrized planar curve is a conjugacy class of an element of $\mathrm{PSL}_2(\mathbb{R})$; these elements are divided into hyperbolic, parabolic, elliptic, and trivial, according to the number of fixed points in $S^1 \simeq \mathbb{RP}^1$ (2, 1, 0, ∞, respectively).

Proposition 4.1. Let $\ell > 0$. Then the ℓ-bicycle monodromy of nS^1, $n \ge 1$, is

- hyperbolic for $\ell < 1$;
- parabolic for $\ell = 1$;
- elliptic for $\ell > 1$, except for the $n - 1$ values

$$\ell_{k,n} = 1\Big/\sqrt{1 - (k/n)^2}, \quad k = 1, 2, \ldots, n-1,$$

for which the monodromy is trivial.

Proof. The ℓ-monodromy of nS^1 is the n-th power of the ℓ-monodromy of the (simple) circle S^1. The latter is easily found by direct calculation to be hyperbolic for $0 < \ell < 1$,

parabolic for $\ell = 1$, and elliptic for $\ell > 1$. The n-th power of hyperbolic or parabolic element is hyperbolic or parabolic, respectively.

An elliptic element is conjugate to a rotation by some angle α, hence its n-th power is trivial if and only if α is a multiple of $2\pi/n$. On the other hand, by Corollary 2.19, α is the solid angle at the vertex of a right cone over S^1 with generator of length ℓ. A simple calculation shows that this solid angle is $2\pi(1 - \sqrt{1 - 1/\ell^2})$. Thus the ℓ-monodromy of nS^1 is trivial if and only if $2\pi(1 - \sqrt{1 - 1/\ell^2}) = 2\pi m/n$ for some $m \in \mathbb{Z}$, or $\ell = 1/\sqrt{1 - (k/n)^2}$, $k = 1, 2, \ldots, n - 1$. ■

Definition 4.2. For each $n \geq 2$ and $1 \leq k \leq n - 1$, let $\Gamma_{k,n}(t)$ be the unique closed plane curve in $2\ell_{k,n}$-bicycle correspondence with nS^1, such that $\Gamma_{k,n}(0) = 1 + 2\ell_{k,n} \in \mathbb{C}$, where $\ell_{k,n} = 1/\sqrt{1 - (k/n)^2}$.

See Figure 21. This class of curves is mentioned in Section 8.4 of [54].

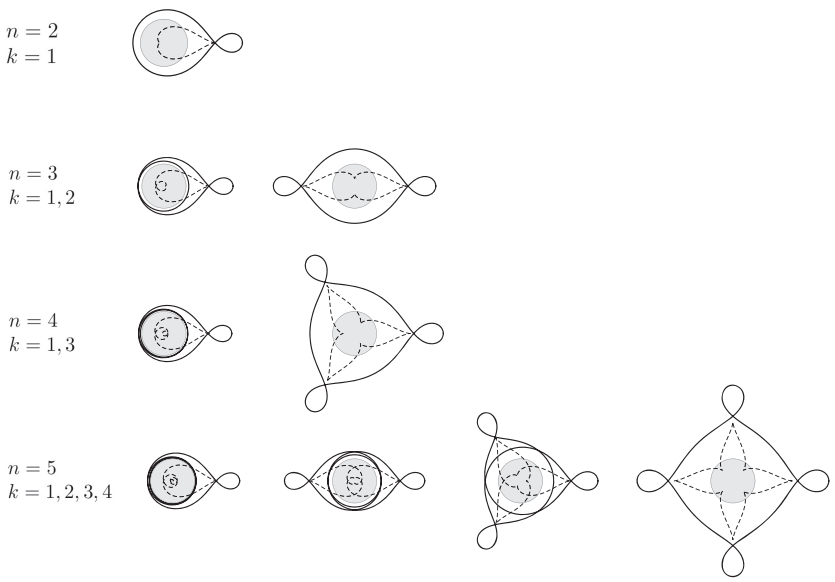

Fig. 21. The curves $\Gamma_{k,n}$ (the solid curves) for $1 \leq k < n \leq 5$ and (k, n) relatively prime. Each one is in bicycle correspondence with the unit circle (the boundary of the gray disk); their common back track is the dotted curve.

Downloaded from https://academic.oup.com/imrn/advance-article-abstract/doi/10.1093/imrn/rny087/4998816 by Pennsylvania State University user on 15 January 2019

Downloaded from https://academic.oup.com/imrn/advance-article-abstract/doi/10.1093/imrn/rny087/4998816 by Pennsylvania State University user on 15 January 2019

Remark 4.3. Since the $\ell_{k,n}$-monodromy of nS^1 is trivial, we have in fact a whole circle worth of planar closed curves in $2\ell_{k,n}$-bicycle correspondence with nS^1. By the obvious rotational symmetry of the bicycle equation for nS^1, they are all obtained from $\Gamma_{k,n}$ by rotation about the origin and shift reparametrization.

We next find an explicit arc length parametrization of $\Gamma_{k,n}$ by solving the bicycle equation for S^1.

Proposition 4.4. One has

$$\Gamma_{k,n}(t) = e^{it}\left[1 + 2\ell e^{i\phi(t)}\right], \tag{58}$$

where $\phi(t)$ is defined (as a continuous function) by

$$\tan\frac{\phi}{2} = -a\tan\frac{bt}{2}, \quad a = \frac{n}{k} + \sqrt{\left(\frac{n}{k}\right)^2 - 1}, \quad b = \frac{k}{n}, \quad \phi(0) = 0. \tag{59}$$

Proof. Let Γ be the unit circle in $\mathbb{R}^2 = \mathbb{C}$, parameterized by $\Gamma(t) = e^{it}$. Let Γ_ℓ be the (not necessarily closed) parameterized plane curve in 2ℓ-bicycle correspondence with Γ, satisfying $\Gamma_\ell(0) = 1 + 2\ell$. By definition, $\Gamma_\ell(t) = \Gamma(t) + 2\ell\mathbf{r}(t)$, where $\mathbf{r}(t)$ is the solution to (4) with $\mathbf{r}(0) = 1 \in \mathbb{C}$. Taking $\Gamma(t) = e^{it}$, $\mathbf{r} = e^{i\theta}$ in (4) gives $\ell\dot\theta = -\cos(\theta - t)$. Changing to $\phi := \theta - t$ gives $\Gamma_\ell(t) = e^{it}\left[1 + 2\ell e^{i\phi(t)}\right]$, where $\phi(t)$ satisfies $\dot\phi = -1 - (\cos\phi)/\ell$, $\phi(0) = 0$. Changing again to $p = \tan(\phi/2)$, gives

$$\dot p = -\frac{1}{2\ell}\left[p^2(\ell - 1) + \ell + 1\right], \quad p(0) = 0,$$

a constant coefficient Riccati equation, whose solution, for $\ell > 1$, is

$$p = -a\tan\frac{bt}{2}, \quad a = \sqrt{\frac{\ell + 1}{\ell - 1}}, \quad b = \sqrt{1 - \frac{1}{\ell^2}}, \quad \ell > 1. \tag{60}$$

For $\ell = \ell_{k,n} = 1/\sqrt{1 - (k/n)^2}$, we obtain the stated formulas. ■

Remark 4.5. There are expressions similar to (60) for Γ_ℓ with $0 < \ell \le 1$ (which we do not really use). For $0 < \ell < 1$,

$$p = -a\tanh\frac{bt}{2},\ a = \sqrt{\frac{1 + \ell}{1 - \ell}},\ b = \sqrt{\frac{1}{\ell^2} - 1}.$$

For $\ell = 1$, we have $\dot p = -1$ so that $p(t) = -t$.

If (k, n) have a common divisor $d > 1$, then $\Gamma_{k,n}$ is a d-fold cover of $\Gamma_{\bar{k},\bar{n}}$, where $\bar{k} = k/d, \bar{n} = n/d$, so all properties of $\Gamma_{k,n}$ can be easily deduced from those of $\Gamma_{\bar{k},\bar{n}}$. We will thus restrict attention henceforth to $\Gamma_{k,n}$ with relatively prime (k, n).

Corollary 4.6. For all $n \geq 2$ and $1 \leq k \leq n-1$,

1. $\Gamma_{k,n}$ and nS^1 have the same length $2\pi n$ and the same λ-bicycle monodromy for all $\lambda > 0$ (as in Proposition 4.1).
2. $\Gamma_{k,n}$ admits a D_k-symmetry (the symmetries of a regular k-gon); that is,

$$\begin{aligned} \Gamma_{k,n}(t + 2\pi n/k) &= e^{2\pi i n/k}\Gamma_{k,n}(t), \\ \Gamma_{k,n}(-t) &= \overline{\Gamma}_{k,n}(t), \end{aligned} \tag{61}$$

for all $t \in \mathbb{R}$.

Proof. The first statement follows from Corollary 3.3 and Theorem 7 and the second from (58) and (59). ■

4.2 $\Gamma_{k,n}$ as Zindler curves

Let $\Gamma(t)$ be an arc length parameterized closed immersed Zindler curve of length L. That is, there is a number $\rho \in (0, 1)$, called a *rotation number* of Γ, such that the chord length $\|\Gamma(t + \rho L) - \Gamma(t)\|$, corresponding to a fixed length ρL of an arc, is a positive constant and the velocity of the midpoint $(\Gamma(t + \rho L) + \Gamma(t))/2$ is parallel to $\Gamma(t + \rho L) - \Gamma(t)$. Note that ρ is a rotation number if and only if so is $1 - \rho$, and that a circle is Zindler for all rotation numbers $\rho \in (0, 1)$.

In this subsection we show that most $\Gamma_{k,n}$ are Zindler and determine their associated rotation numbers (Theorem 10). The proof, although elementary, is somewhat technical, so we give here the main idea.

By construction, each $\Gamma_{k,n}$ is in bicycle correspondence with nS^1, hence its λ-bicycle monodromy is hyperbolic for $0 < \lambda < 1$ and parabolic for $\lambda = 1$. It follows that for all $\lambda \leq 1$ there is a planar closed curve $\Gamma^{\lambda}_{k,n}$ in 2λ-bicycle correspondence with $\Gamma_{k,n}$ (unique up to reflection about one of the symmetry axes of $\Gamma_{k,n}$). By Bianchi permutability and circular symmetry, each $\Gamma^{\lambda}_{k,n}$ is a rigid rotation of $\Gamma_{k,n}$ about the origin by some λ-dependent angle χ. By the D_k-symmetry of $\Gamma_{k,n}$ (Corollary 4.6), if χ is a multiple of $2\pi/k$ then $\Gamma^{\lambda}_{k,n}$ coincides with $\Gamma_{k,n}$ (up to shift reparametrization), so that $\Gamma_{k,n}$ is Zindler.

Downloaded from https://academic.oup.com/imrn/advance-article-abstract/doi/10.1093/imrn/rny087/4998816 by Pennsylvania State University user on 15 January 2019

Downloaded from https://academic.oup.com/imrn/advance-article-abstract/doi/10.1093/imrn/rny087/4998816 by Pennsylvania State University user on 15 January 2019

Thus the proof of the Zindler property of $\Gamma_{k,n}$ and the calculation of the associated rotation numbers reduce to the calculation of χ as a function of $\lambda \in (0,1]$. This is done in Lemma 4.7 and is the main ingredient in the proof of Theorem 10. (In fact, it is more convenient to write $\lambda = \sin(\gamma/2)$ and calculate χ as a function of $\gamma \in (0,\pi]$.)

Theorem 10. Let (k, n) be a relatively prime pair of positive integers. Then $\Gamma_{k,n}$ is a Zindler curve if and only if $1 \leq k \leq n-2$, with $n-k-1$ rotation numbers $\rho \in (0,1)$, given by the equation

$$n \tan(k\pi\rho) = k \tan(n\pi\rho) \tag{62}$$

(including $\rho = 1/2$ when both n and k are odd).

Proof. For each $\ell > 0$, $\gamma \in (0,\pi]$ and $t \in \mathbb{R}$, define

- $\Gamma(t) = e^{it}$,
- $\Gamma^\lambda(t) = e^{i(t+\gamma)}$, where $\lambda = \sin(\gamma/2) \in (0,1]$,
- $\Gamma_\ell(t)$—the (not necessarily closed) 2ℓ-bicycle transform of $\Gamma(t)$ with $\Gamma_\ell(0) = 1 + 2\ell \in \mathbb{C}$,
- $\Gamma^\lambda_\ell(t)$—the completion of $\Gamma^\lambda(t)\Gamma(t)\Gamma_\ell(t)$ to the Darboux Butterfly $\Gamma^\lambda(t)\Gamma(t)\Gamma_\ell(t)$ $\Gamma^\lambda_\ell(t)$.

Note that Γ^λ is in 2λ-bicycle correspondence with Γ and so, by Bianchi permutability (Proposition 3.8), Γ^λ_ℓ is in 2λ-bicycle correspondence with Γ_ℓ, as well as 2ℓ-bicycle correspondence with Γ^λ. It follows (see Remark 4.3) that there exist $\chi, \tau \geq 0$ such that

$$\Gamma^\lambda_\ell(t) = e^{-i\chi}\Gamma_\ell(t+\tau) \tag{63}$$

for all t. See Figure 22.

Lemma 4.7. For $\ell > 1$, $\chi(\gamma)$ and $\tau(\gamma)$ in (63) satisfy

$$\tan\left(\frac{b\tau}{2}\right) = b \tan\frac{\gamma}{2}, \quad \chi = \tau - \gamma, \quad b = \sqrt{1 - \frac{1}{\ell^2}}.$$

It follows that χ is a monotonically increasing function of γ, varying from 0 to $\pi(1/b-1)$, as γ varies from 0 to π.

■

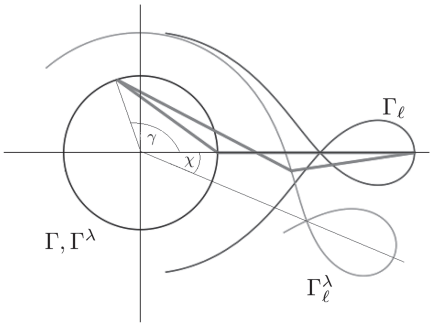

Fig. 22. The notation of the proof of Theorem 10.

Proof. By definition, we have

$$\Gamma_\ell(t) = e^{it}(1 + 2\ell e^{i\phi(t)}),$$

where $\phi(t)$ is given by (60), and

$$\Gamma_\ell^\lambda(t) = e^{it}(e^{i\gamma} + 2\ell e^{i\psi(t)}),$$

for some function $\psi(t)$. Substituting the last two equations in (63), we get

$$e^{i(\gamma+\chi)} + 2\ell e^{i[\psi(t)+\chi]} = e^{i\tau} + 2\ell e^{i[\phi(t+\tau)+\tau]}.$$

Both sides of the last equation are parameterized arcs of circles of radius 2ℓ, hence their centers and angular parameter must coincide, giving

$$\tau = \chi + \gamma, \quad \psi(t) = \phi(t + \tau) + \gamma.$$

Note that, strictly speaking, these equations hold only modulo 2π, but by the continuous dependence of τ, χ, and ψ on γ, and the initial conditions $\tau(0) = \chi(0) = \psi(0) = 0$, they hold as stated.

This gives the stated second formula and $\psi(0) = \phi(\tau) + \gamma$, hence

$$\tan\frac{\psi(0)}{2} = \tan\left(\frac{\phi(\tau)}{2} + \frac{\gamma}{2}\right) = \frac{\tan\frac{\phi(\tau)}{2} + \tan\frac{\gamma}{2}}{1 - \tan\frac{\phi(\tau)}{2}\tan\frac{\gamma}{2}}.$$

Downloaded from https://academic.oup.com/imrn/advance-article-abstract/doi/10.1093/imrn/rny087/4998816 by Pennsylvania State University user on 15 January 2019

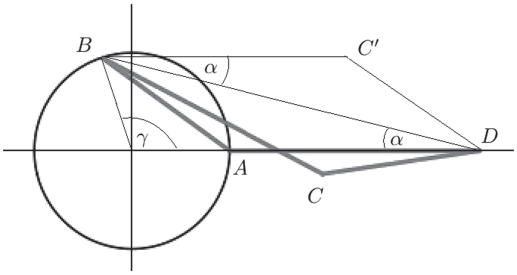

Fig. 23. The Darboux Butterfly *ABCD*.

Using (60), we get from the last equation

$$\tan\frac{\psi(0)}{2}=\frac{-a\tan\frac{b\tau}{2}+\tan\frac{\gamma}{2}}{1+a\tan\frac{b\tau}{2}\tan\frac{\gamma}{2}},\qquad a=\sqrt{\frac{1+\ell}{1-\ell}}. \tag{64}$$

Next, we look at the Darboux Butterfly *ABCD*, where $A=\Gamma(0)=1$, $B=\Gamma^{\lambda}(0)=e^{i\gamma}$, $C=\Gamma^{\lambda}_{\ell}(0)=e^{i\gamma}+2\ell e^{i\psi(0)}$, and $D=\Gamma_{\ell}(0)=1+2\ell$. See Figure 23.

Let C' be the reflection of C about BD. Then $ABC'D$ is a parallelogram, in which $\alpha=\angle DBC'=\angle BDA=-\psi(0)/2$, $AD=2\ell$, $AB=2\lambda$, and $\angle ABD=\pi/2-\alpha-\gamma/2$. Applying the sine law to $\triangle DAB$, we get

$$\frac{\sin(\pi/2-\alpha-\gamma/2)}{2\ell}=\frac{\sin\alpha}{2\lambda}.$$

Using $\lambda=\sin(\gamma/2)$ and solving the last equation for $\tan\alpha$, we get

$$-\tan\frac{\psi(0)}{2}=\tan\alpha=\frac{\tan(\gamma/2)}{\ell+(\ell+1)\tan^2(\gamma/2)}.$$

Substituting this into the left hand side of (64) and simplifying, we obtain the stated formula $\tan(b\tau/2)=b\tan(\gamma/2)$. It follows immediately from this formula that

$$\chi'(\gamma)=\tau'(\gamma)-1=\frac{u^2}{\ell^2(1+b^2u^2)},$$

where $u=\tan^2(\gamma/2)$, hence χ (as well as τ) is monotonically increasing in γ, as stated. ■

Downloaded from https://academic.oup.com/imrn/advance-article-abstract/doi/10.1093/imrn/rny087/4998816 by Pennsylvania State University user on 15 January 2019

We continue with the proof of Theorem 10. Setting $\ell = \ell_{k,n} = 1/\sqrt{1-(k/n)^2}$ in Lemma 4.7, we have $b = k/n$, so that

$$n \tan \frac{k}{n}\frac{\tau}{2} = k \tan \frac{\gamma}{2}, \tag{65}$$

and $\chi = \tau - \gamma$ increases monotonically from 0 to $\pi(n-k)/k$, as γ varies from 0 to π.

Now the Zindler condition on $\Gamma_{k,n}$ is that it is in the bicycle correspondence with itself (up to shift reparametrization). Due to the D_k-symmetry (see Corollary 4.6), this means that χ in (63) should be an integer multiple of $2\pi/k$. As γ varies from 0 to π, χ increases monotonically from 0 to $\pi(n-k)/k$, so there are exactly $[(n-k)/2]$ values $\gamma \in (0,\pi]$ for which χ is an integer multiple of $2\pi/k$. For each such γ, $\Gamma_{k,n}$ is Zindler with chord length $2\lambda = 2\sin(\gamma/2)$, giving rise to a pair of rotation numbers $\{\rho, 1-\rho\} \subset (0,1)$, except if $\rho = 1/2$, which occurs if and only if $\gamma = \pi$ and $n-k$ is even (i.e., k, n are both odd). It follows that $\Gamma_{k,n}$ is Zindler if and only if $1 \le k \le n-2$, with a total of $n-k-1$ rotation numbers $\rho \in (0,1)$, as stated.

To determine the associated rotation numbers, let γ be a value for which

$$\chi = 2\pi m/k, \quad m = 1, 2, \ldots, [(n-k)/2]. \tag{66}$$

An associated rotation number $\rho \in (0,1)$ satisfies

$$\Gamma^{\lambda}_{k,n}(t) = \Gamma_{k,n}(t + 2\pi n\rho) \tag{67}$$

for all t. Since k, n are relatively prime, there exists an integer $\bar{n}$ such that $n\bar{n} \equiv 1 \pmod{k}$. Let $\bar{m} := m\bar{n}$, then

$$\frac{2\pi m}{k} \equiv \frac{2\pi \bar{m} n}{k} \pmod{2\pi}. \tag{68}$$

Now we calculate

$$\begin{aligned}
\Gamma^{\lambda}_{k,n}(t) &= e^{-i\frac{2\pi m}{k}}\Gamma_{k,n}(t+\tau) && \text{by (63),(66)}\\
&= e^{-i\frac{2\pi \bar{m} n}{k}}\Gamma_{k,n}(t+\tau) && \text{by (68)}\\
&= \Gamma_{k,n}\left(t + \tau - \frac{2\pi \bar{m} n}{k}\right) && \text{by (61)}\\
&= \Gamma_{k,n}(t + 2\pi n\rho) && \text{by (67)}
\end{aligned} \tag{69}$$

Downloaded from https://academic.oup.com/imrn/advance-article-abstract/doi/10.1093/imrn/rny087/4998816 by Pennsylvania State University user on 15 January 2019

for all t. The last equality is equivalent to $\tau - 2\pi\bar{m}n/k \equiv 2\pi n\rho \pmod{2\pi n}$, implying

$$\frac{k}{n}\frac{\tau}{2} \equiv \pi k\rho \pmod{\pi}. \tag{70}$$

Next, applying $2\ell_{k,n}$-bicycling correspondence to (67) gives $\Gamma^{\lambda}(t) = \Gamma(t + 2\pi n\rho)$ or $e^{i(t+\gamma)} = e^{i(t+2\pi n\rho)}$. It follows that $\gamma \equiv 2\pi n\rho \pmod{2\pi}$ or

$$\frac{\gamma}{2} \equiv \pi n\rho \pmod{\pi}. \tag{71}$$

Substituting (70) and (71) in (65), we see that ρ satisfies (62).

We have shown so far that $\Gamma_{k,n}$ has $n - k - 1$ rotation numbers and that they all satisfy equation (62). To complete the proof of Theorem 10 it is thus sufficient to show that equation (62) has exactly $n - k - 1$ solutions $\rho \in (0, 1)$ (including $\rho = 1/2$, when k, n are both odd).

Lemma 4.8. For any pair of integers k, n with $1 \le k < n$, equation (62)

$$n\tan(k\pi\rho) = k\tan(n\pi\rho)$$

has $n - k - 1$ solutions in $(0, 1)$, including $\rho = 1/2$ when both n and k are odd.

Proof. Clearly, ρ is a solution if and only if

$$\left(\frac{1}{n\pi}\right)\arctan\left(\frac{n}{k}\tan(k\pi\rho)\right) \equiv \rho \pmod{\frac{1}{n}}.$$

For each $j \in \mathbb{Z}$, let $I_j = (j/k - 1/2k, j/k + 1/2k) \subset \mathbb{R}$ (the open interval of length $1/k$ centered at j/k) and define $f_j : I_j \to \mathbb{R}$ by

$$f_j(\rho) := \left(\frac{1}{n\pi}\right)\arctan\left(\frac{n}{k}\tan(k\pi\rho)\right) + \frac{j}{n}, \quad \rho \in I_j, \quad j \in \mathbb{Z}.$$

One can verify that f_j extends smoothly to $\bar{I}_j$ and that the extensions at adjacent intervals coincide at the shared endpoints, combining to define a smooth, strictly increasing function $f : \mathbb{R} \to \mathbb{R}$, satisfying

(i) $f(0) = 0$,
(ii) $f(1) = k/n$, and

Downloaded from https://academic.oup.com/imrn/advance-article-abstract/doi/10.1093/imrn/rny087/4998816 by Pennsylvania State University user on 15 January 2019

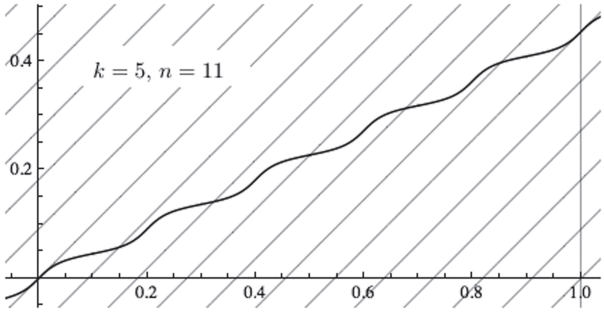

Fig. 24. The function $f(\rho)$ of the proof of Lemma 4.8.

(iii) $0 < f'(\rho) \leq 1$ for all $\rho \in \mathbb{R}$, with $f'(\rho) = 1$ only at isolated points. (In fact, $f'(\rho) = 1$ precisely at $\rho \equiv 0 \pmod{1/k}$.)

See Figure 24. By construction, the solutions of equation (62) are given by

$$f(\rho) \equiv \rho \pmod{\frac{1}{n}}.$$

It now follows easily from the above three properties of f that this equation has exactly $n - k - 1$ solutions in the interval $0 < \rho < 1$. ■

This concludes the proof of Theorem 10.

Remark 4.9.

(i) Here is a table of the (approximate) rotation numbers $\rho \in (0, 1/2]$ of $\Gamma_{k,n}$, for relatively prime pairs (k, n), with $1 \leq k \leq n - 2$ and $n \leq 7$.

k	n	ρ
1	3	0.5
1	4	0.37
1	5	0.29, 0.5
2	5	0.31
3	5	0.5
1	6	0.24, 0.41

k	n	ρ
1	7	0.21, 0.35, 0.5
2	7	0.21, 0.37
3	7	0.23, 0.5
4	7	0.35
5	7	0.5

Downloaded from https://academic.oup.com/imrn/advance-article-abstract/doi/10.1093/imrn/rny087/4998816 by Pennsylvania State University user on 15 January 2019

(ii) Here is also a plot of all rotation numbers for $n = 11$.

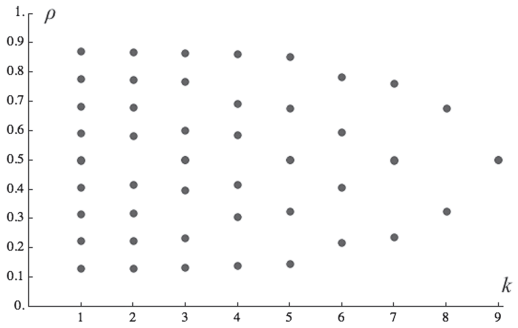

(iii) For small values of (k, n), the numbers $\tan^2(\pi\rho)$ are roots of linear or quadratic polynomials, obtained from multiple angle trigonometric identities. Here are all such cases with $\rho \neq 1/2$:

k	n	$\tan^2(\pi\rho)$
1	4	5
1	5	$5/3$
2	5	$2\sqrt{21} - 7$
1	6	$\left(21 \pm 4\sqrt{21}\right)/3$
1	7	$\left(7 \pm 2\sqrt{7}\right)/3$

For higher values of (k, n), the numbers $\tan^2(\pi\rho)$ are roots of higher degree polynomials.

(iv) For $k = 1$, (62) is $n\tan(\pi\rho) = \tan(n\pi\rho)$. This is equation (14) of Theorem 7 of [46], describing the rotation numbers ρ for which the (simple) unit circle can be infinitesimally deformed in the class of planar Zindler curves with rotation number ρ.

The same equation appeared in a study of billiards and of a flotation problem [21, 22]. See [13] for number theoretic properties of its solutions. A discrete version of the equation is proposed in [46]; see [11, 12] for its solutions.

Downloaded from https://academic.oup.com/imrn/advance-article-abstract/doi/10.1093/imrn/rny087/4998816 by Pennsylvania State University user on 15 January 2019

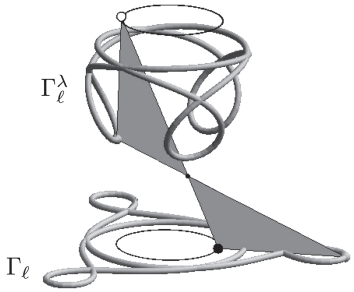

Fig. 25. The spherical curve Γ_ℓ^λ.

4.3 Spherical curves in bicycle correspondence with $\Gamma_{k,n}$

As we have seen in the previous subsection, all curves in 2λ-bicycle correspondence with $\Gamma_{k,n}$, for $\lambda \leq 1$, are rotations of $\Gamma_{k,n}$ about the origin. For a generic value of $\lambda > 1$ (i.e., for $\lambda \neq \ell_{k',n}$, $1 \leq k' < n$), the λ-monodromy of $\Gamma_{k,n}$ is elliptic, and thus there are two space curves in 2λ-bicycle correspondence with $\Gamma_{k,n}$, related by reflection about the xy-plane.

Proposition 4.10. Let $\lambda > 1$ and let $\Gamma_{k,n}^\lambda$ be a curve in $\mathbb{R}^3$ in 2λ-bicycle correspondence with $\Gamma_{k,n}$. Then $\Gamma_{k,n}^\lambda$ is either planar, contained in the xy plane, in which case $\lambda = \ell_{k',n}$ for some $1 \leq k' < n$, or it is a spherical curve, with the center of the sphere on the z axis.

Proof. We define for every $\ell > 0$, $\lambda > 1$, and $t \in \mathbb{R}$:

- $\Gamma(t) = (e^{it}, 0) \in \mathbb{C} \oplus \mathbb{R} = \mathbb{R}^3$ (lower thin circle in Figure 25),
- $\Gamma^\lambda(t) = (e^{-it}, 2\sqrt{\lambda^2 - 1})$ (upper thin circle),
- $\Gamma_\ell(t)$—the (not necessarily closed) curve in the xy-plane in 2ℓ-bicycle correspondence with Γ, such that $\Gamma_\ell(0) = (1 + 2\ell, 0, 0) \in \mathbb{R}^3$ (lower thick planar curve),
- $\Gamma_\ell^\lambda(t)$—the completion of $\Gamma^\lambda(t)\Gamma(t)\Gamma_\ell(t)$ to the Darboux Butterfly $\Gamma^\lambda(t)\Gamma(t)\Gamma_\ell(t)$ $\Gamma_\ell^\lambda(t)$ (upper thick space curve).

Note that Γ is in 2λ-bicycle correspondence with Γ^λ and in 2ℓ-bicycle correspondence with Γ_ℓ, and hence, by Bianchi permutability, Γ_ℓ^λ is in 2λ-bicycle correspondence with Γ_ℓ and in 2ℓ-bicycle correspondence with Γ^λ. Since Γ^λ is related to Γ by Euclidean translation along the z-axis and reparametrization, it is enough to show that any curve (not necessarily closed) in 2ℓ-bicycle correspondence with Γ lies either in the xy plane or on some sphere centered on the z-axis.

Downloaded from https://academic.oup.com/imrn/advance-article-abstract/doi/10.1093/imrn/rny087/4998816 by Pennsylvania State University user on 15 January 2019

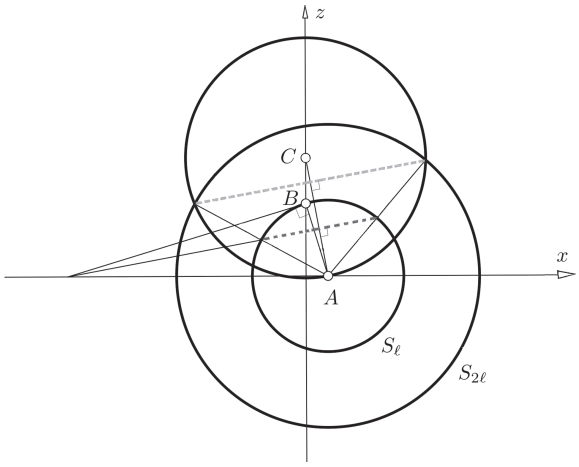

Fig. 26. The proof of Proposition 4.10.

At this junction, we can explicitly solve the bicycle equation, as described in Section 2.4: this is an equation with constant coefficients. We present a more geometrical argument here.

The desired property is invariant with respect to rotations about the z-axis, so it can be shown in a frame rotating about the z-axis with angular velocity 1.

In this frame, the front wheel $\Gamma(t)$ is stationary, say at $A = (1, 0, 0)$, so the rear wheel traces some curve on the two-sphere S_ℓ of radius ℓ centered at A. We claim that this curve is a circle (shown as a dotted chord of S_ℓ in Figure 26), whose axis (the line through its center, perpendicular to the plane of the circle) intersects the z axis at some point C, or else is parallel to the z-axis, in which case the curve is the equatorial circle (the intersection of S_ℓ with the xy-plane).

Indeed, the bicycle equation (4) in a rotating frame (the Frenet–Serret frame) is autonomous, that is, defines a time-independent conformal vector field on S_ℓ, whose flow is a one-parameter elliptic subgroup of the Möbius group of S_ℓ (here we use the fact that $\ell > 1$). Its trajectories are planar circles, with two fixed points, the vertices of the two right circular cones over Γ with generator of length ℓ; one of them, B, is shown in Figure 26.

It follows that the curve in 2ℓ-bicycle correspondence with Γ, generated by this rear track (shown as a dotted chord of $S_{2\ell}$ in Figure 26), is a circle on the sphere $S_{2\ell}$ of radius 2ℓ, centered at A, as well as a circle on the sphere centered at C and passing through A. ■

Downloaded from https://academic.oup.com/imrn/advance-article-abstract/doi/10.1093/imrn/rny087/4998816 by Pennsylvania State University user on 15 January 2019

A Bicycle correspondence as a Darboux transformation

In this appendix we relate the bicycle correspondence for curves in $\mathbb{R}^3$ with Darboux transformations of a certain spectral problem.

We use the STP construction (after Sym, Tafel, and Pohlmeyer), associating with each solution of the AKNS system a family of curves in $\mathfrak{su}_2 \cong \mathbb{R}^3$. We note that only Theorem 12 of this section is new; the preliminary material, as well as related motivation and details, can be found in [40]. The curves that we are dealing with in this subsection are not necessarily closed.

We begin with a description of the *AKNS system*, following [4]. Given a complex-valued function $q(t)$ of a real variable t, we define the linear system

$$\Phi_t = (Q + i\lambda A)\Phi, \tag{A.1}$$

where $\Phi = \Phi(t, \lambda)$ is a complex 2×2 matrix-valued function of two real variables, $\Phi_t = \partial\Phi/\partial t$ and

$$Q = \begin{pmatrix} 0 & q \\ -\bar{q} & 0 \end{pmatrix}, \quad q = q(t), \quad A = \begin{pmatrix} \frac{1}{2} & 0 \\ 0 & -\frac{1}{2} \end{pmatrix}.$$

The variable λ is called the *spectral parameter* and Q is the *potential*. Observe that $Q + i\lambda A$ is $\mathfrak{su}_2$-valued, hence if we assume, as we shall do henceforth, that

$$\Phi(0, \lambda) \in \mathrm{SU}_2 \ \textit{for all} \ \lambda \in \mathbb{R},$$

then $\Phi(t, \lambda) \in \mathrm{SU}_2$ for all (t, λ) as well.

Given a solution $\Phi(t, \lambda)$ to (A.1), we define, following [45], the associated STP curves $\Gamma(t, \lambda)$ in $\mathfrak{su}_2$ by

$$\Gamma = \Phi^* \Phi_\lambda. \tag{A.2}$$

In what follows, we use the (slightly modified) standard Killing form on $\mathfrak{su}_2$, $\|X\|^2 = -2\mathrm{tr}(X^2)$.

Proposition A.1. For each λ, the map $t \mapsto \Gamma(t, \lambda)$ defines an arc length parameterized curve in $\mathfrak{su}_2$, that is, $\|\Gamma_t\| = 1$, with the curvature and torsion functions given in terms of $q(t)$ by

$$\kappa = 2|q|, \quad \tau = \mathrm{Im}\,(q_t/q) - \lambda. \tag{A.3}$$

Downloaded from https://academic.oup.com/imrn/advance-article-abstract/doi/10.1093/imrn/rny087/4998816 by Pennsylvania State University user on 15 January 2019

Downloaded from https://academic.oup.com/imrn/advance-article-abstract/doi/10.1093/imrn/rny087/4998816 by Pennsylvania State University user on 15 January 2019

Conversely, given a curve C in $\mathfrak{su}_2$ with curvature κ and torsion τ, the AKNS system associated with

$$q = \frac{\kappa}{2} e^{i\int \tau}$$

has a family of STP curves $\Gamma(\cdot, \lambda)$ with curvature κ and torsion $\tau - \lambda$, so that $\Gamma(\cdot, 0)$ is congruent to C. In fact, by adjusting the initial condition $\Phi(0, \lambda)$ in (A.1), one can have $\Gamma(\cdot, 0)$ actually coincide with C.

Proof. A simple calculation shows that $\Gamma = \Phi^* \Phi_\lambda$ implies $\Gamma_t = \Phi^*(iA)\Phi$. Since the Killing form is conjugation-invariant, $\|\Gamma_t\|^2 = \|iA\|^2 = 1$. Similarly, one finds that $\Gamma_{tt} = \Phi^*[iA, Q]\Phi$ and

$$\Gamma_{ttt} = \Phi^* \left([iA, Q_t] + [[iA, Q], Q + i\lambda A] \right) \Phi,$$

from which follows

$$\kappa = \|\Gamma_{tt}\| = \|[iA, Q]\| = 2|q|$$

and

$$\tau = \frac{\langle [\Gamma_t, \Gamma_{tt}], \Gamma_{ttt} \rangle}{\kappa^2} = \operatorname{Im}(q_t/q) - \lambda.$$

Conversely, given a curve C in $\mathfrak{su}_2$ with curvature and torsion functions κ, τ, one can verify easily that $q = (\kappa/2)e^{i\int \tau}$ satisfies (A.3) for $\lambda = 0$, so that the STP curve $\Gamma(\cdot, \lambda)$, associated with the AKNS system defined by q, has curvature κ and torsion $\tau - \lambda$.

Finally, if we take a solution $\Phi(t, \lambda)$ to the AKNS system (A.1) and right-multiply it by $G(\lambda) \in \mathrm{SU}_2$, then we obtain another solution of (A.1), whose STP curve is $G^* \Gamma G + G^* G_\lambda$. The first term is a rotation of Γ and the second gives a translation, so that by choosing G appropriately we can move $\Gamma(\cdot, 0)$ onto C. ■

Next, we define the *Darboux transformations* of the AKNS system (A.1). To this end, we fix a *non-real* complex number μ and a nonzero element $v \in \mathbb{C}^2$ and use the data (μ, v) to transform the AKNS system (A.1) to a new system $\tilde{\Phi}_t = (\tilde{Q} + i\lambda A)\tilde{\Phi}$, where $\tilde{Q}$ and $\tilde{\Phi}$ are given in terms of Q, Φ and (μ, v), as follows. Let

$$\phi(t) = \begin{pmatrix} \phi_1(t) \\ \phi_2(t) \end{pmatrix}$$

be the $\mathbb{C}^2$-valued function defined by

$$\phi_t = (Q + i\mu A)\phi, \quad \phi(0) = v,$$

and the associated projection operator

$$\pi = \frac{\phi\phi^*}{\|\phi\|^2} = \frac{1}{|\phi_1|^2 + |\phi_2|^2} \begin{pmatrix} \phi_1\bar{\phi}_1 & \phi_1\bar{\phi}_2 \\ \phi_2\bar{\phi}_1 & \phi_2\bar{\phi}_2 \end{pmatrix}.$$

Note that $\pi(t)$ is the orthogonal projection on the (complex) one-dimensional subspace of $\mathbb{C}^2$ spanned by $\phi(t)$, hence it is unchanged if v is multiplied by a nonzero complex scalar.

Next, define the complex numbers

$$\alpha = \sqrt{\frac{\lambda - \bar{\mu}}{\lambda - \mu}}, \quad \beta = \frac{\mu - \bar{\mu}}{\lambda - \bar{\mu}},$$

and the linear operators

$$U = \alpha(I - \beta\pi), \quad \tilde{Q} = Q + i(\mu - \bar{\mu})[A, \pi], \tag{A.4}$$

where $[A, \pi] = A\pi - \pi A$.

Lemma A.2.

1. $U(t, \lambda) \in \mathrm{SU}_2$.
2. $\tilde{Q}(t) \in \mathfrak{su}_2$ is the potential associated with the complex function

$$\tilde{q} = q + i(\mu - \bar{\mu})\frac{\bar{\phi}_1\phi_2}{\|\phi\|^2}.$$

Proof.

1. π is an orthogonal projection operator, hence is conjugate, by some element in SU_2, to $diag(1, 0)$. It follows that U is conjugate, by the same element, to $diag(\alpha(1 - \beta), \alpha)$, from which it follows that $U(t, \lambda) \in \mathrm{SU}_2$.
2. One calculates that

$$[A, \pi] = \frac{1}{\|\phi\|^2} \begin{pmatrix} 0 & \phi_1\bar{\phi}_2 \\ -\bar{\phi}_1\phi_2 & 0 \end{pmatrix},$$

from which the stated formula follows easily. ■

The following theorem shows how the Darboux transformation $Q \mapsto \tilde{Q}$ is matched by a transformation $\Phi \mapsto \tilde{\Phi}$ of the solutions to the associated AKNS systems.

Downloaded from https://academic.oup.com/imrn/advance-article-abstract/doi/10.1093/imrn/rny087/4998816 by Pennsylvania State University user on 15 January 2019

Downloaded from https://academic.oup.com/imrn/advance-article-abstract/doi/10.1093/imrn/rny087/4998816 by Pennsylvania State University user on 15 January 2019

This is followed by a description of the effect of the transformation on the associated curves in $\mathbb{R}^3$.

Theorem 11. ([40]) Φ is a solution to the AKNS system (A.1) if and only if $\tilde{\Phi} := U\Phi$ is a solution to the AKNS system

$$\tilde{\Phi}_t = (\tilde{Q} + i\lambda A)\tilde{\Phi}, \tag{A.5}$$

where $U, \tilde{\Phi}$ are given by (A.4) above.

The proof is by a straighforward calculation using the formulas above and is omitted.

Now we look at the effect of the Darboux transformation $\Phi \mapsto \tilde{\Phi}$ on the associated STP curves.

Proposition A.3. Let $\tilde{\Gamma} = \tilde{\Phi}^*\tilde{\Phi}_\lambda$. Then

$$\tilde{\Gamma} - \Gamma = \frac{\mu - \bar{\mu}}{|\lambda - \mu|^2}\Phi^*\left(\pi - \frac{1}{2}I\right)\Phi, \qquad \|\tilde{\Gamma} - \Gamma\| = \frac{|\mu - \bar{\mu}|}{|\lambda - \mu|^2}. \tag{A.6}$$

In particular, the distance $\|\tilde{\Gamma}(t,\lambda) - \Gamma(t,\lambda)\|$ is independent of t.

Proof. The formula for $\tilde{\Gamma} - \Gamma$ is a direct calculation using the definitions above and is omitted. To calculate $\|\tilde{\Gamma} - \Gamma\|$, note that π, being an orthogonal projection, is conjugate by an element in SU_2 to $diag(1, 0)$, thus $i\left(\pi - \frac{1}{2}I\right)$ is conjugate by the same element to iA, which is of unit norm. This implies the stated formula. ■

The last proposition states that the pair of STP curves $\Gamma(\cdot,\lambda), \tilde{\Gamma}(\cdot,\lambda)$ satisfy one of the conditions needed to be in bicycle correspondence. To get the other condition, one needs to restrict μ and λ.

Theorem 12. If we choose a purely imaginary $\mu = i\varepsilon$ in the Darboux transformation described above and $\lambda = 0$, then the pair of $\mathfrak{su}_2$-valued curves Γ and $\tilde{\Gamma}$ are in $2/|\varepsilon|$-bicycle correspondence.

Conversely, let Γ_1, Γ_2 be two parametrized curves in $\mathbb{R}^3$ in 2ℓ-bicycle correspondence. Then, there exists an AKNS system (A.1) with initial conditions $\Phi(0,\lambda) \in SU_2$ whose corresponding STP curve at $\lambda = 0$ is Γ_1, and a Darboux transform with $\mu = i/\ell$ mapping Γ_1 to Γ_2.

Proof. Consider a Darboux transformation with $\mu = i\varepsilon$ and associated STP curves $\Gamma, \tilde{\Gamma}$. Let $W = \tilde{\Gamma} - \Gamma$. By Proposition A.3, $\|W\| = 2/|\varepsilon|$. What is left to show then is that W and $(\Gamma_t + \tilde{\Gamma}_t)/2$ are parallel for $\lambda = 0$, that is, $[W, \Gamma_t + \frac{1}{2}W_t] = 0$. The proof is by a simple but lengthy computation. We omit the details.

Conversely, given two curves Γ_1, Γ_2 in $\mathfrak{su}_2$ in 2ℓ-bicycling correspondence, let κ_1 and τ_1 be the curvature and torsion functions of Γ_1. According to Proposition A.1, the AKNS system associated with $q = (\kappa_1/2)e^{i\int \tau_1}$, with appropriate initial conditions, realizes Γ_1 as the associated STP curve at $\lambda = 0$. We now show that an appropriate Darboux transformation maps Γ_1 to Γ_2.

From the first part of the theorem, we know that Darboux transformations with $\mu = i/\ell$ produce curves in 2ℓ-bicycle correspondence with Γ_1. We use the expression for $\tilde{\Gamma} - \Gamma$ in formula (A.6) of Proposition A.1 to show that, by varying $v \in \mathbb{C}^2 \setminus \{0\}$, we obtain *all* curves in 2ℓ-bicycling correspondence with Γ_1 and, in particular, Γ_2. By this formula, the direction of $\tilde{\Gamma} - \Gamma$ at $t = 0$ is the unit vector

$$B(v) := i\left(\frac{vv^*}{\|v\|^2} - \frac{1}{2}I\right) \in \mathfrak{su}_2,$$

rotated by conjugation with Φ. Now the map $v \mapsto B(v)$ is clearly SU_2-equivariant, $B(gv) = gB(v)g^{-1}$. Its image is therefore the whole unit sphere in $\mathfrak{su}_2$ (the orbit of iA under SU_2).

It follows that every initial direction of $\tilde{\Gamma} - \Gamma$ at $t = 0$ can be obtained by choosing v appropriately; consequently, we obtain all curves Γ_2 in 2ℓ-bicycle correspondence with Γ_1. ∎

B Proof of Proposition 3.15

We will prove the statement of Proposition 3.15 for a class of ODEs (ordinary diferential equations) that includes the bicycle Riccati equation (46). For each C^∞ function $f : \mathbb{C} \times \mathbb{R} \to \mathbb{C}$, complex analytic in the first variable and T-periodic in the second, consider the ODE

$$\dot{Z} = -\frac{1}{\ell}Z + f(Z, t), \tag{B.1}$$

where $\dot{Z} = \partial_t Z$. (Note that (46) converts to this form upon the change of variable $t \mapsto -t$, which interchanges stable and unstable fixed points.) We will show the following.

Proposition B.1. For every function $f : \mathbb{C} \times \mathbb{R} \to \mathbb{R}$ as above, there exists an $\ell_0 > 0$ such that for every $0 < \ell < \ell_0$

(1) there is a unique periodic solution $Z(t, \ell)$ to (B.1) with $|Z(t, \ell)| < 1$ for all t.

Downloaded from https://academic.oup.com/imrn/advance-article-abstract/doi/10.1093/imrn/rny087/4998816 by Pennsylvania State University user on 15 January 2019

(2) $Z(t, \ell)$ is a stable periodic solution.

(3) Extended to $\ell = 0$ as $Z(t, 0) \equiv 0$, $Z(t, \ell)$ is infinitely differentiable in $\mathbb{R} \times [0, \ell_0)$. In particular, $\lim_{\ell \downarrow 0} \partial_t^n Z(t, \ell) = 0$ and $\partial_\ell^n Z(t, 0)$ exist for all $t \in \mathbb{R}$ and integer $n \geq 0$.

Note that the above existence result implies immediately the uniqueness statement in Proposition 3.15, since a Möbius transformation in $\mathrm{PSL}_2(\mathbb{C})$ has at most one unstable fixed point. We divide the proof into the following steps.

1. There exists an $\ell_0 > 0$ (depending on f alone) such that for all $0 < \ell < \ell_0$ the period map $\varphi : \mathbb{C} \to \mathbb{C}$ of (B.1) has a unique fixed point in $\mathrm{D} := \{|Z| \leq 1\}$. This fixed point is stable and the associated periodic solution $Z(t, \ell)$ is C^∞ in $\mathbb{R} \times (0, \ell_0)$.
2. For all integers $n \geq 0$:
$$\lim_{\ell \downarrow 0} \partial_t^n Z(t, \ell) = 0. \tag{B.2}$$
3. For all integers $n \geq 0$, the limit
$$a_n(t) := \lim_{\ell \downarrow 0} \partial_\ell^n Z(t, \ell) \tag{B.3}$$
exists.
4. $Z(t, \ell)$, extended to $\ell = 0$ by $Z(t, 0) = 0$, is C^∞ in $\mathbb{R} \times [0, \ell_0)$ with $\partial_\ell^n Z(t, 0) = a_n(t)$.

Step 1. Let $M = \max |f(Z, t)|$ over $|Z| \leq 1$ and $t \in \mathbb{R}$, and let $\ell_1 > 0$ be such that $1/\ell_1 > M$. Then, for all $\ell < \ell_1$, if $Z(t)$ is a solution to (B.1) and $|Z(t)| = 1$ for some t, one has
$$\frac{1}{2} \frac{d}{dt} |Z|^2 = Z \cdot \dot{Z} \overset{\text{(B.1)}}{=} -\frac{1}{\ell} |Z|^2 + f \cdot Z \leq -\frac{1}{\ell} + \frac{1}{\ell_1} < 0. \tag{B.4}$$
It follows that for $\ell < \ell_1$ the period map φ maps D into itself, and thus has a fixed point.

To prove uniqueness we show that, for ℓ small enough, φ resricted to D is a contraction. For this, it is enough to show that $|\varphi'(Z_0)| \leq \rho$ for some $\rho < 1$ and all $Z_0 \in \mathrm{D}$. This will show also that the fixed point is stable.

Choose an arbitrary solution $Z(t)$ of (B.1) with $Z(0) \in \mathrm{D}$ and consider a nontrivial solution $U(t)$ of the linearized equation $\dot{U} = -\frac{1}{\ell} U + f_Z U$ around $Z(t)$; here $f_Z = \partial_Z f(Z, t)$. The derivative of the period map φ at $Z(0)$ is given by
$$\varphi'(Z(0)) = \frac{U(T)}{U(0)} = \exp \int_0^T \left(-\frac{1}{\ell} + f_Z \right) \mathrm{d}t.$$

Downloaded from https://academic.oup.com/imrn/advance-article-abstract/doi/10.1093/imrn/rny087/4998816 by Pennsylvania State University user on 15 January 2019

Now, given $\varepsilon > 0$, there exists $\ell_0 < \ell_1$ such that $\mathrm{Re}\left(-\frac{1}{\ell} + f_Z\right) < -\varepsilon$ for all $\ell \le \ell_0$, hence $|\varphi'(Z(0))| \le e^{-T\varepsilon} < 1$, proving that φ is a contraction in D. Since φ is analytic, and the contraction is by a factor bounded away from 1, we conclude that the fixed point is an analytic function of ℓ for all $0 < \ell < \ell_0$.

Step 2. We prove (B.2) by induction on n. For $n = 0$, it suffices to show that for $\ell < \ell_1$, our periodic solution satisfies $|Z(t,\ell)| \le \ell/\ell_1$. If $|Z(t,\ell)| > \ell/\ell_1$ for some t, then (for this t), by (B.4),

$$\frac{1}{2}\frac{d}{dt}|Z|^2 = -\frac{1}{\ell}|Z|^2 + f \cdot Z \le \left(-\frac{1}{\ell}|Z| + \frac{1}{\ell_1}\right)|Z| < 0. \tag{B.5}$$

It follows that for all $\ell < \ell_1$ the periodic solution $Z(t, \ell)$ is confined to the disk $|Z| \le \ell/\ell_1$ and thus $\lim_{\ell\downarrow 0} Z(t,\ell) = 0$. This completes the step $n = 0$ of the induction.

Assume now that (B.2) holds up to order $n - 1$ for some $n > 0$. Let us denote $Y_k := \partial_t^k Z$. Differentiating (B.1) n times by t, we obtain

$$\dot{Y}_n = -\frac{1}{\ell}Y_n + \partial_t^n f.$$

The last term is of the form

$$\partial_t^n f = AY_n + B_n,$$

where $A = f_Z(Z(t,\ell),t)$ and where B_n is a polynomial in the variables $Z, Y_1, \ldots, Y_{n-1}$ (containing no Y_n) with coefficients of the form $\partial_Z^i \partial_t^j f(Z,t)$ with $i + j \le n$. By the assumption on f, these coefficients are bounded. This and the inductive assumption imply that

$$\lim_{\ell\downarrow 0} A = f_Z(0,t), \quad \lim_{\ell\downarrow 0} B_n = B_n^0, \tag{B.6}$$

where $B_n^0 = B_n^0(t)$ is a smooth function. Summarizing, Y_n satisfies the ODE

$$\dot{Y}_n = \left(-\frac{1}{\ell} + A\right)Y_n + B_n \tag{B.7}$$

with the coefficients satisfying (B.6). The same argument used in proving that $\lim_{\ell\downarrow 0} Z = 0$ applies here, and it shows that $\lim_{\ell\downarrow 0} Y_n = 0$. This completes the proof of (B.2).

Step 3. We prove (B.3) by induction on n. For $n = 0$, we already proved it in Step 2. For any fixed $n > 0$, assume that (B.3) holds for all orders $< n$. Let $Z_k = \partial_\ell^k Z$. Multiplying both sides of (B.1) by ℓ and differentiating n times with respect to ℓ, we get

$$\ell\dot{Z}_n + n\dot{Z}_{n-1} = -Z_n + \partial_\ell^n(\ell f). \tag{B.8}$$

Downloaded from https://academic.oup.com/imrn/advance-article-abstract/doi/10.1093/imrn/rny087/4998816 by Pennsylvania State University user on 15 January 2019

Downloaded from https://academic.oup.com/imm/advance-article-abstract/doi/10.1093/imm/my087/4998816 by Pennsylvania State University user on 15 January 2019

Now

$$\partial_\ell^n(\ell f(Z,t)) = \ell\partial_\ell^n f + n\partial_\ell^{n-1} f = \ell A Z_n + \ell C_n + n\partial_\ell^{n-1} f,$$

where, similarly to Step 3, we have $A = f_Z$ and C_n is a polynomial in $Z, Z_1, \dots Z_{n-1}$ with coefficients of the form $\partial_Z^j f(Z,t)$ with $j \le n$. By Step 3,

$$\lim_{\ell\downarrow 0} A \stackrel{def}{=} f_Z(0,t) \stackrel{def}{=} A^0,$$

and by the inductive assumption,

$$\lim_{\ell\downarrow 0} C_n \stackrel{def}{=} C_n^0$$

exists. Substituting all this into (B.8) yields, after some manipulation,

$$\dot{Z}_n = -\frac{\alpha}{\ell}\,(Z_n - \beta)\,, \tag{B.9}$$

where

$$\alpha = 1 - \ell A, \quad \beta = \frac{n\partial_\ell^{n-1} f - n\dot{Z}_{n-1} + \ell C_n}{\alpha}.$$

We have $\lim_{\ell\downarrow 0}\alpha = 1$; to show that $\lim_{\ell\downarrow 0}\beta$ exists, we need to know that $\dot{Z}_{n-1}$ has a limit as $\ell \downarrow 0$. We showed that this limit exists for $\dot{Z}_0 = \dot{Z}$; let us add the inductive assumption to the one already made that $\lim_{\ell\downarrow 0}\dot{Z}_{n-1}$ exists; we will show in a moment that then $\lim_{\ell\downarrow 0}\dot{Z}_n$ exists as well. With this assumption,

$$\lim_{\ell\downarrow 0}\beta = n\lim_{\ell\downarrow 0}\left(\partial_\ell^{n-1} f - \dot{Z}_{n-1}\right)$$

exists. To complete the induction we must show that the limits of Z_n and of $\dot{Z}_n$ exist. The existence of these limits follows from (B.9) and from the existence of the limits of α and β; we will in fact show that

$$\lim_{\ell\downarrow 0} Z_n = \lim_{\ell\downarrow 0}\beta,$$

and

$$\lim_{\ell\downarrow 0}\dot{Z}_n = \lim_{\ell\downarrow 0}\dot{\beta}. \tag{B.10}$$

Indeed,

$$\frac{1}{2}\frac{d}{dt}(Z_n-\beta)^2 \stackrel{(B.9)}{=} -\frac{\alpha}{\ell}(Z_n-\beta)^2 - \dot{\beta}\cdot(Z_n-\beta),$$

which shows that $|Z_n - \beta|$ is monotonically decreasing whenever $|Z_n - \beta| \geq 2\max|\dot{\beta}|\ell$. This shows that our periodic Z_n is confined to $|Z_n - \beta| < 2\max|\dot{\beta}|\ell$ (by the argument used in Step 3), and thus converges to β as $\ell \downarrow 0$, as claimed.

Finally, differentiating (B.9) by t, one can apply a similar Lyapunov–type argument to prove the existence of the limit in (B.10). This completes the induction step and thus the proof of (B.3).

Step 4. Consider the difference quotient

$$\frac{Z_n(t,\ell) - Z_n(t,0)}{\ell} = \frac{1}{\ell}\int_0^\ell Z_{n+1}(t,s)\,\mathrm{d}s,$$

where $Z_n(t,0)$ is the limit which exists by Step 3. Since also $\lim_{\ell\downarrow 0} Z_{n+1}(t,\ell)$ exists, so does the limit of the above integral, showing that

$$\lim_{\ell\downarrow 0}\frac{Z_n(t,\ell) - Z_n(t,0)}{\ell} = Z_{n+1}(t,0),$$

and thus proving the claim. ■

Funding

This work was supported by Conacyt [grant 222870 to G. B.]; Shapiro Visitor Program [to R. P.]; and by National Science Foundation [DMS-1412542 to M. L., DMS-1510055 to S. T.].

Acknowledgments

We thank R. Montgomery, J. Langer, L. Hernández, and F. Wegner for inspiring discussions, and S. Wagon for great help with Mathematica. G.B. and R.P. are grateful to the Department of Mathematics of Penn State for its hospitality. We also thank one of the referees for very extensive and helpful comments and suggestions.

References

[1] Arreaga, G., R. Capovilla, C. Chryssomalakos, and J. Guven. "Area-constrained planar elastica." *Phys. Rev. E* 65, no. 3 (2002): 031801.

[2] Arnold, V. "The geometry of spherical curves and quaternion algebra." *Russian Math. Surveys* 50 (1995): 1–68.

[3] Arnold, V. and B. Khesin. *Topological Methods in Hydrodynamics*. New York: Springer, 1998.

[4] Ablowitz, M., D. Kaup, A. Newell, and H. Segur. "The inverse scattering transform-Fourier analysis for nonlinear problems." *Stud. Appl. Math.* 53 (1974): 249–315.

[5] Auerbach, H. "Sur un problème de M. Ulam concernant l'èquilibre des corps flottants." *Studia Math* 7 (1938): 121–42.

Downloaded from https://academic.oup.com/imrn/advance-article-abstract/doi/10.1093/imrn/rny087/4998816 by Pennsylvania State University user on 15 January 2019

[6] Bracho, J., L. Montejano, and D. Oliveros. "A classification theorem for Zindler carrousels." *J. Dyn. Control Systems* 7 (2001): 367–84.

[7] Bracho, J., L. Montejano, and D. Oliveros. "Carousels, Zindler curves and the floating body problem." *Period. Math. Hungar.* 49 (2004): 9–23.

[8] Benedetti, R. and R. Petronio. *Lectures on Hyperbolic Geometry*. Berlin: Springer, 1992.

[9] Bryant, R. "Intuition for the Cartan connection and "Rolling without slipping" in Cartan geometry". URL (version: 2016–01-29): http://mathoverflow.net/q/229569.

[10] Bryant, R. and L. Hsu. "Rigidity of integral curves of rank 2 distributions." *Invent. Math.* 114 (1993): 435–61.

[11] Csikós, B. "On the rigidity of regular bicycle (n, k)-gons." *Contrib. Discrete Math.* 2 (2007): 93–106.

[12] Connelly, R. and B. Csikós. "Classification of first-order flexible regular bicycle polygons." *Studia Sci. Math. Hungar.* 46 (2009): 37–46.

[13] Cyr, V. "A number theoretic question arising in the geometry of plane curves and in billiard dynamics." *Proc. Amer. Math. Soc.* 140 (2012): 3035–40.

[14] Djondjorov, P., V. Vassilev, and I. Mladenov. "Analytic description of the equilibrium shapes of elastic rings under uniform hydrostatic pressure." *Int. Workshop on Complex Structures, Integrability and Vector Fields*, 189–202. *AIP Conf. Proc.* 1340. *Amer. Inst. Phys.*, Melville, NY, 2011.

[15] Finn, D. "Can a bicycle create a unicycle track?" *College Math. J.* 33 (2002): 283–92.

[16] Finn, D. "Which way did you say that bicycle went?" *Math. Mag.* 77 (2004): 357–67.

[17] Foote, R. "Geometry of the Prytz planimeter." *Rep. Math. Phys.* 42 (1998): 249–71.

[18] Foote, R., M. Levi, and S. Tabachnikov. "Tractrices, bicycle tire tracks, hatchet planimeters, and a 100-year-old conjecture." *Amer. Math. Monthly* 120 (2013): 199–216.

[19] Fukumoto, Y. and M. Miyajima. "The localized induction hierarchy and the Lund-Regge equation." *J. Phys. A* 29 (1996): 8025–34.

[20] Greenhill, A. G. "The elastic curve under uniform normal pressure." *Math. Ann.* 52.4 (1889): 465–500.

[21] Gutkin, E. "Billiard Tables of Constant Width and Dynamical Characterization of the Circle." Proc. Workshop on Dynamics and Related Topics, 1993: 24–24 Penn. State Univ., PA, 1993.

[22] Gutkin, E. "Capillary floating and the billiard ball problem." *J. Math. Fluid Mech.* 14 (2012): 362–82.

[23] Gutkin, E. "Addendum to: capillary floating and the billiard ball problem." *J. Math. Fluid Mech.* 15 (2013): 425–30.

[24] Halphen, G. H. *La corbe élastique plane sous pression uniforme, Chap. V in Traité des fonctions elliptiques et de leurs applications. Deuxième partie: Applications a la mécanique, a la physique, a la géodésie, a la géométrie et au calcul intégral*. Paris: Gauthier-Villars et fils, 1888.

[25] Hasimoto, H. "A soliton on a vortex filament." *J. Fluid Mech.* 51 (1972): 477–85.

[26] Hill, F. W. "The hatchet planimeter." *Proc. Physical Soc. London* 13, no. 1 (1894): 229–34.

[27] Howe, S., M. Pancia, and V. Zakharevich. "Isoperimetric inequalities for wave fronts and

Downloaded from https://academic.oup.com/imrn/advance-article-abstract/doi/10.1093/imrn/rny087/4998816 by Pennsylvania State University user on 15 January 2019

a generalization of Menzins conjecture for bicycle monodromy on surfaces of constant curvature." *Adv. Geom* 11 (2011): 273–92.

[28] Ince, E. L. *Ordinary Differential Equations*. New York: Dover Publications, 1978.

[29] Langer, J. "Recursion in curve geometry." *New York J. Math.* 5 (1999): 25–51.

[30] Langer, J. and R. Perline. "Poisson geometry of the filament equation." *J. Nonlinear Sci.* 1 (1991): 71–93.

[31] Langer, J. and R. Perline. "The planar filament equation." *Mechanics day (Waterloo, ON, 1992)*, 171–180. *Fields Inst. Commun.* 7. *Amer. Math. Soc.* Providence, RI, 1996.

[32] Levi, M. "Composition of rotations and parallel transport." *Nonlinearity* 9 (1996): 413–9.

[33] Levi, M. ""Bike tracks," quasi-magnetic forces, and the Schrödinger equation." *SIAM News* 47 (2014).

[34] Levi, M. "Schrödinger's equation and "bike tracks" - a connection." *J. Geom. Phys.* 115 (2017): 124–30.

[35] Levi, M. and S. Tabachnikov. "On bicycle tire tracks geometry, hatchet planimeter, Menzin's conjecture, and oscillation of unicycle tracks." *Exp. Math.* 18 (2009): 173–86.

[36] Lévy, M. M. "Mémoire sur un nouveau cas intégrable du probléme de l'élastique et l'une de ses applications." *J. Math. Pures Appl. sér.* 3 X (1884): 5–42.

[37] Levy, S. and W. P. Thurston. *Three-dimensional Geometry and Topology*, vol. 1. Providence, RI: Princeton Univ. Press, 1997.

[38] Mackenzie, D. "Following in Sherlock Holmes' Bike Tracks." In *What's Happening in the Mathematical Sciences* 10, 52–63. Providence, RI: AMS, 2015.

[39] Marsden, J. and A. Weinstein. "Coadjoint orbits, vortices, and Clebsch variables for incompressible fluids." *Phys. D* 7 (1983): 305–23.

[40] Rogers, C. and W. Schief. *Bäcklund and Darboux Transformations*. Cambridge: Cambridge University Press, 2002.

[41] Ruban, A. "Sur le problème du cylindre flottant." *Dokl. Akad. Nauk* 25 (1939): 350–2.

[42] Salgaller, V. and P. Kostelianetz. "Sur le problème du cylindre flottant." *Dokl. Akad. Nauk* 25 (1939): 353–5.

[43] *The Scottish Book. Mathematics from the Scottish Café*. Edited by R. D. Mauldin. Boston, Mass.: Birkhäuser, 1981.

[44] Singer, D. "Lectures on elastic curves and rods." *Curvature and variational modeling in physics and biophysics*, 3–32. *AIP Conf. Proc.* 1002. *Amer. Inst. Phys.* Melville, NY, 2008.

[45] Sym, A. "Soliton surfaces and their applications (soliton geometry from spectral problems)." *Geometric aspects of the Einstein equations and integrable systems (Scheveningen, 1984)*, 154–231. *Lecture Notes in Phys.* 239. Berlin: Springer, 1985.

[46] Tabachnikov, S. "Tire track geometry: variations on a theme." *Israel J. Math.* 151 (2006): 1–28.

[47] Tabachnikov, S. and E. Tsukerman. "On the discrete bicycle transformation." *Publ. Mat. Urug.* 14 (2013): 201–19.

[48] Tabachnikov, S. "On the bicycle transformation and the filament equation: results and conjectures." *J. Geom. Phys.* 115 (2017): 116–23.

Downloaded from https://academic.oup.com/imrn/advance-article-abstract/doi/10.1093/imrn/rny087/4998816 by Pennsylvania State University user on 15 January 2019

[49] Veiro, J. P. "Octonionic presentation for the Lie group $SL_2(\mathbb{O})$." *J. Algebra Appl.* 13 (2014): 1450017, 19.

[50] Wegner, F. "Floating bodies of equilibrium." *Stud. Appl. Math.* 111 (2003): 167–83.

[51] Wegner, F. "Floating bodies of equilibrium I." Preprint 2002, arXiv:physics/0203061.

[52] Wegner, F. "Floating bodies of equilibrium II." Preprint 2002, arXiv:physics/0205059.

[53] Wegner, F. "Floating bodies of equilibrium. Explicit solution." Preprint 2006, arXiv:physics/0603160.

[54] Wegner, F. "Floating bodies of equilibrium in 2D, the tire track problem and electrons in a parabolic magnetic field." Preprint 2007, arXiv:physics/0701241.

[55] Wegner, F. "Three problems - one solution." http://www.tphys.uni-heidelberg.de/~wegner/Fl2mvs/Movies.html.

[56] Zindler, K. "Über konvexe Gebilde II." *Monatsh. Math. Phys.* 31 (1921): 25–57.

Downloaded from https://academic.oup.com/imrn/advance-article-abstract/doi/10.1093/imrn/rny087/4998816 by Pennsylvania State University user on 15 January 2019